2008

COLOR MULTIPLEXED SINGLE PATTERN SLI

Neelima Mandava
University of Kentucky, Neelima.Mandava@gmail.com

ABSTRACT OF THESIS

COLOR MULTIPLEXED SINGLE PATTERN SLI

Structured light pattern projection techniques are well known methods of accurately capturing 3-Dimensional information of the target surface. Traditional structured light methods require several different patterns to recover the depth, without ambiguity or albedo sensitivity, and are corrupted by object movement during the projection/capture process. This thesis work presents and discusses a color multiplexed structured light technique for recovering object shape from a single image thus being insensitive to object motion.

This method uses single pattern whose RGB channels are each encoded with a unique subpattern. The pattern is projected on to the target and the reflected image is captured using high resolution color digital camera. The image is then separated into individual color channels and analyzed for 3-D depth reconstruction through use of phase decoding and unwrapping algorithms thereby establishing the viability of the color multiplexed single pattern technique. Compared to traditional methods (like PMP, Laser Scan etc) only one image/one-shot measurement is required to obtain the 3-D depth information of the object, requires less expensive hardware and normalizes albedo sensitivity and surface color reflectance variations. A cosine manifold and a flat surface are measured with sufficient accuracy demonstrating the feasibility of a real-time system.

KEYWORDS: Structured Light Illumination, Single Pattern, Color, Phase, 3D.

Neelima Mandava

December, 8th 2008

COLOR MULTIPLEXED SINGLE PATTERN SLI

By,

Neelima Mandava

Dr. Laurence G Hassebrook
Director of Thesis

Dr. YuMing Zhang
Director of Graduate Studies

December, 8th 2008

RULES OF THE THESIS

Unpublished theses submitted for the Master's degree and deposited in the University of Kentucky Library are as a rule open for inspection, but are to be used only with due regard to the rights of the authors. Bibliographical references may be noted, but quotations or summaries of parts may be published only with the permission of the author, and with the usual scholarly acknowledgments.

Extensive copying or publication of the thesis in whole or in part also requires the consent of the Dean of the Graduate School of the University of Kentucky.

A library that borrows this thesis for use by its patrons is expected to secure the signature of each user.

Name Date

_____

_____

_____

_____

_____

_____

_____

_____

_____

THESIS

Neelima Mandava

The Graduate School

University of Kentucky

2008

COLOR MULTIPLEXED SINGLE PATTERN SLI

THESIS

A thesis submitted in partial fulfillment of the requirements for the degree of Master of Science in Electrical Engineering in the College of Engineering at the University of Kentucky

By

Neelima Mandava
Lexington, Kentucky

Director: Dr. Laurence G. Hassebrook, Professor of Electrical Engineering
Lexington, Kentucky
2008

DEDICATION

My Parents

ACKNOWLEDGEMENTS

First of all I would take this valuable opportunity to express my sincere thanks and gratitude to my advisor and mentor Dr. Laurence Hassebrook. He has always been very supportive with constant guidance and valuable suggestions enabling me achieve my academic goals. I'm also grateful to each of the professors, staff members, and my co-students who have helped me to get to this point. I would like to thank my family, my father, Mr. Sambasiva Rao Mandava with his never ending faith in me has been my ideal inspiration providing constant encouragement and motivation at every step of my life. My mother Ramadevi Mandava, there never has been any woman so caring and loving as her, thank you for your unconditional love and support. My Sister and brother-in-law for their friendly support and caring. A special thanks my husband Mr. Srujan Potluri for his support and love. I would like to thank Charles Casey and all other batch mates for all their cooperation and help. I would like to thank my friends Sandhya and Pallavi for their support and best wishes. Finally, I would also like to thank my committee professors Dr. Kevin Donohue and Dr. Ruigang Yang for their time and aid.

TABLE OF CONTENTS

LIST OF TABLES

LIST OF FIGURES

LIST OF FILES

Neelima_Mandava_Thesis.pdf……4.2MB

Chapter 1 Introduction

1.1 Motivation and Objective

3-D shape measurements using optical triangulation techniques provide non-contact surface measurement and thus have many applications in the fields of quality control, robotics, medical diagnostics, computer vision , etc[1-3]. Out of two dominate triangulation techniques namely passive stereo vision and active structured light illumination researchers have been motivated towards increasingly active methods because of their higher accuracy in measurements. Structured light illumination alleviate major drawback of passive stereo vision techniques, i.e. correspondence problem between both image planes [4] and low texture environmental conditions. Structured light illumination simplifies the problem by using a light source which projects a known pattern of light on the object being measured. The depth modified patterns are then analyzed to measure a particular topology of the object. The various devices that are used for structured light noncontact measurement are cameras, projectors, computer, etc. Various developments in the field of cameras, Optics and computer software have made 3D depth data acquisition yield better results in practice. The main working principle that makes the depth measurement by SLI possible is known as Optical Triangulation [4]. The basic SLI system consists of a single camera and digital projector with their respective optical axis aligned [9]. The projector projects a light pattern which can be single stripe, multi stripe, single spot, binary, gray code, sine wave or any arbitrary pattern, on to a target surface [5]. By measuring the distortion between the captured and the reflected image, the depth information can be extracted. Traditional SLI techniques use multi-patterns for reliable and accurate reconstruction but this slows down the acquisition speed [9]. Necessity of capturing multiple-frames to produce a single 3D image can introduce serious errors in measurement due to motion introduced by target between successive frames. Popular multi-pattern SLI technique like phase measuring profilometry (PMP) have good measurement accuracy but take more time to scan the target object and thus capture rate can’t be achieved at video rate. Another significant drawback of multi-

pattern techniques is the difficulty to use high resolution digital cameras which require the image to be captured with a single shot. This makes them unsuitable for faster scans using digital cameras. In order to be able to speed up the data acquisition process researchers have tried various approaches that require smaller number of projection patterns or more specifically a single pattern [13]. Single-pattern techniques are current state of art in 3D data acquisition systems. They are sometimes called one-shot systems, as they are able to extract the depth data from a single gray-level or color snapshot of the scene. With single pattern techniques use of high pixel cameras digital cameras is very feasible for image capturing. Single patterns can effectively retrieve 3-D shape reconstruction at the frame rate of the camera. There are two broad categories of one shot systems, the first one uses a black-and-white projection patterns [12-14].The main advantage of a black-and-white approach is that it works well, even with a wide range of colored scenes. The downside of the black-and-white single pattern systems is their coarse lateral resolution, and sensitivity to surface albedo variations. The second category of one shot systems uses color single pattern techniques that employ three separate color channels which can potentially provide triple transmission capacity over black-and-white projection patterns and use different patterns in each color channel to reduce sensitivity to albedo variance. Thus, color projection patterns tend to achieve a much higher lateral resolution of the depth data. However, the colors reflected from a scene strongly depend on its intrinsic reflectivity, implying that the colors seen by the camera can differ substantially from the originally projected ones. Most single pattern color-based coded light systems simply equate the former with the latter limiting them to scenes with neutral colors [19–20].

With this motivation we designed the color multiplexed pattern that uses a combination of three primary color channels Red, green and blue to code the light patterns for 3-D shape measurement. Since color multiplexed technique is based on single pattern projection it has the advantage of working with high resolution digital cameras and single shot image capture thus suitable for measuring static and dynamic scenes. The emphasis is given to Red and Green color channels in the projected color stripe pattern to reduce surface reflectance since many objects and subjects of interest

like human skin work well because they don't contain very much blue. Ratio based measurement of red and green channel intensities are used to give uninterrupted phase information and to overcome albedo sensitivity problem. In order to deal with correspondence problem, we projected color patterns which can effectively encode more bits of information. The main goal of this thesis work is to see how much information can be retrieved from color-space. A 3-D data calibration process is done as part of experimentation for accurate reconstruction.

1.2 Thesis Organization

The thesis consists of five chapters, Appendix and References section. Chapter 1 discusses the motivation and objective of the research work. Chapter 2 gives background for SLI technique and a detailed literature is presented. Also various Multi-pattern and Color single Pattern techniques with their advantages and disadvantages are discussed. Chapter 3 explains the design of color multiplexing single pattern technique, develops mathematical basis. We also describe the algorithmic implementation procedure for analyzing and processing captured data for phase calculation, unwrapping the phase for 3-D reconstruction. Chapter 4 includes the experimental results obtained at each stage of processing of the color pattern. The error analysis for the results is performed and methods employed to correct the errors are explained along with improved results. It also describes the calibration and experimental setup and results of the 3D reconstruction of the target obtained by using color multiplexed single pattern technique. Chapter 5 provides a concluding overview of the thesis by presenting the problems observed and suggests possible courses of future work. Appendix section includes the assumptions and critical code used in the research work. And the references include study material referred.

Chapter 2 Literature Review and Background

3D Data acquisition involves determining the 3-D surface coordinates in three dimensions such as Euclidean $\{X_w, Y_w, Z_w\}$ space. Fig 2.1 shows the taxonomy [11] of the 3D depth scanning or shape acquisition techniques. The 3D shape acquisition techniques can be broadly classified as contact and non-contact methods of acquisition. Optical 3D surface scanning techniques can be further classified into passive and active approaches. The major distinction between these two is that the passive approaches are based upon the measurement of the radiation already present in the scene while the active approaches emit energy into the scene [1].

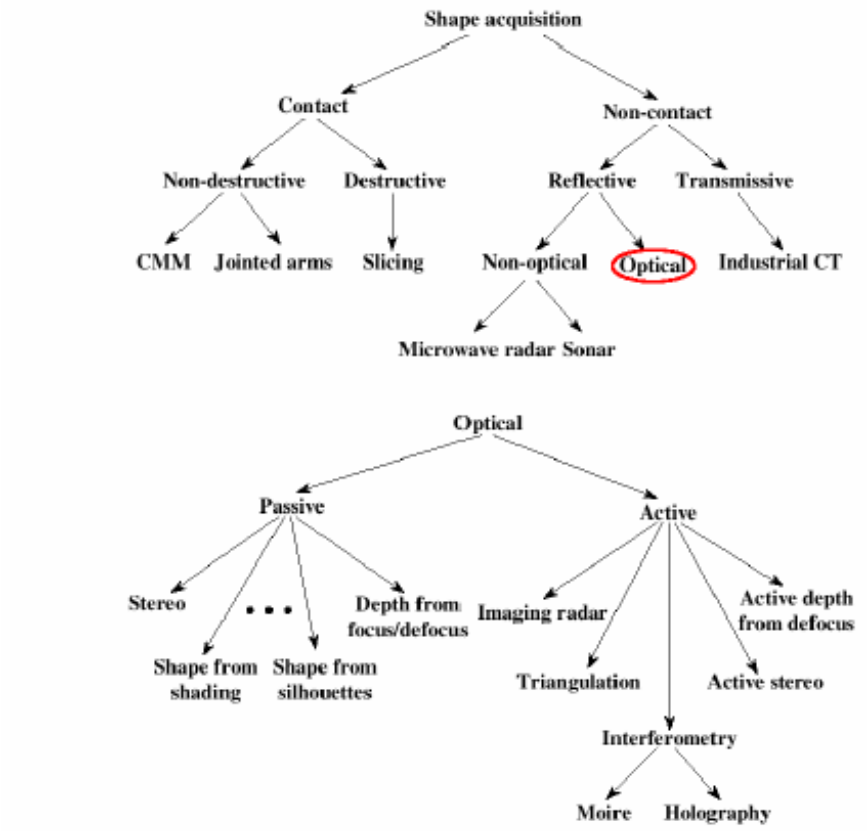

Figure 2. 1 Taxonomy of 3D shape acquisition systems [11]

Structured light illumination (SLI) techniques provide useful means by which data about 3D surface can be acquired without contacting the surface and hence fall under the category of non-contact active vision methods of data acquisition. When compared to the other optical passive techniques like stereo vision and shape-from-x (x-shading, texture, shadow, motion) [9] SLI techniques overcome the fundamental ambiguities which

generally occur in low texture environments and also facilitate non-contact surface measurement. This is quite useful in engineering and industrial applications involving defect detection, accurate mounting of IC chips on to a circuit board, quality control, obstacle avoidance in robot navigation and 3D teleconferencing [1].

2.1 SLI General principle

SLI works on the optical triangulation principle [4]. In this process we project a series of patterns on to the surface of the object using projector such that, when viewed from an angle, the reflected light from the surface appears to the camera to be laterally offset according to the depth of the object. The light pattern can be a single light spot, a stripe or some complex light pattern. The Fig 2.2 illustrates the principle of optical triangulation. The location of the center of the reflected light imaged on the sensor corresponds to a line of sight that intersects the illuminant in exactly one point, yielding a depth value. The depth information can be calculated by estimating the lateral shift caused by the depth. The key advantage of SLI technique is that the camera captured patterns are encoded with projector coordinates such that the correspondence matching only involves decoding of the captured image.

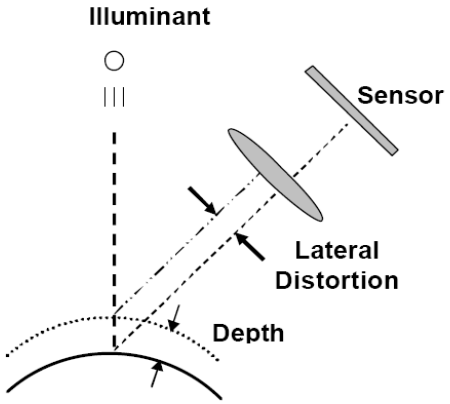

Figure 2. 2 Basic Principle of Optical Triangulation [11]

Classical 3-D acquisition devices use a single scanning laser stripe scanned progressively over the surface of the target object, placing burden on the object to remain static during the entire scan. These traditional SLI techniques are inappropriate for real time applications where the goal is to track continuous motion in a dynamic scene. To reduce the technological burdens of scanning and processing each scan position of the laser stripe, many methods such as multiple light striped patterns or sinusoidal grating patterns, illuminate the entire target surface in one instant have been devised [8]. But they suffer from drawbacks such as introducing ambiguities in surface reconstruction around surface discontinuities, overly sensitive to surface reflectance called albedo variations and also suffer from low lateral resolution caused by the required spacing between stripes and hence cannot be used for real-time imaging. The solution to the ambiguity and albedo problem is to encode the surface repeatedly with multiple light striped patterns. The pattern projection methods have the property of nondestructive detection, faster measurement speed etc [14]. Also by using triangulation and suitable calibration methods the distribution of projected pattern is analyzable to obtain 3D data information efficiently.

2.2 Multi Pattern SLI Techniques

One effective solution to overcome ambiguity in phase measurements and albedo problem is to use multiple light striped patterns with variable spatial frequencies commonly referred to as multi-pattern techniques. Phase Measuring Profilometry (PMP) [11] is a form of temporal multi-pattern projection. Temporal based encoding techniques project a sequence of patterns with different number of stripes on to the surface and the intensity of the stripes is coded uniquely. Thus system measurement can be accomplished with just one pixel location [10]. It has several advantages including its pixel-wise calculation, resistance to ambient light and resistance to reflectance variation.

2.2.1 Traditional PMP method

In PMP, [9] the light pattern consists of a gray level field which varies sinusoidally. In each subsequent projection, the field is spatially shifted in the direction of variation for one sinusoidal period. Due to the continuously varying nature of the pattern, each projector row or column may be encoded uniquely and identified according to the equation

$$I_n^p(x^p, y^p) = A^p + B^p \cos(2\pi f_\Phi y^p - 2\pi n/N) \quad (2.1)$$

Where A^p and B^p are constants of the projector, f_Φ is the frequency of the sine wave, and (x^p, y^p) is the projector coordinate. The y^p dimension is in the direction of the depth distortion and is called the phase dimension. On the other hand, x^p dimension is perpendicular to the phase dimension and called orthogonal dimension [9]. The frequency f_Φ of the sinusoid wave is in the phase direction. Sinusoid patterns are projected and shifted by a factor of $2\pi n/N$ for N times. The subscript n represents the phase shift index and $n = 0, 1\ldots. (N-1)$ where N is the total number of phase shifts.

The reflected intensity images from the object surface after successive projections are viewed distorted by camera as

$$I_n(x^c, y^c) = \alpha(x^c, y^c).[A + B\cos(2\pi f_\Phi y^p + \Phi(x^c, y^c) - 2\pi n/N)] \quad (2.2)$$

Where (x^c, y^c) are the image coordinates and $\alpha(x^c, y^c)$ is the reflectance variation or the albedo. The phase distortion $\Phi(x^c, y^c)$ of the sinusoid wave corresponds to the object surface depth. The value of $\Phi(x^c, y^c)$ is determined from the captured patterns by [9]

$$\Phi(x^c, y^c) = \arctan\left[\frac{\sum_{n=1}^{N} In(x^c, y^c)\sin(2\pi n/N)}{\sum_{n=1}^{N} In(x^c, y^c)\cos(2\pi n/N)}\right] \quad (2.3)$$

The albedo, $\alpha(x^c, y^c)$ is cancelled in this calculation, therefore, the depth through this approach is independent of the albedo. From the eqs (1) and (2) the projector coordinate y^p can be recovered as

$$y^p = \Phi(x^c, y^c)/2\pi f \quad (2.4)$$

Once the phase is obtained, the depth of the objects can be easily obtained by a geometric computation. The base frequency is the *f* that gives 1 cycle across the field of view and therefore yields a no ambiguous depth value.

The single frequency PMP technique is not quite suitable for reliable 3D data acquisition. The scan time, in other words, the total number of phase shifted patterns projected is directly proportional to the quality of 3D data acquired**.** Also the depth measurement accuracy increases with the number of shifts. Recently [9] Li, Hassebrook and Guan in their work have extended single frequency PMP technique to incorporate multiple sinusoidal frequencies. This multi-frequency PMP has the advantage of higher accuracy for a given number of frames and, equivalently, fewer necessary frames for any desired scan accuracy with respect to standard PMP. By adding a second frequency they have proved that the 3D data acquired is less noisy and hence, the reconstruction is better.

2.2.2 Multi-Frequency PMP

Multi-frequency PMP [10] is derived from the single frequency PMP technique. The total scan time is also limited to a fixed value. This implies that the total number of phase shifted patterns projected will be a constant in spite of using multiple frequencies. Compared with other SL algorithms like light stripe, binary bar, and Gray-code projection, PMP uses fewer number of frames, has higher precision, and higher computational efficiency. But all the temporal based multiplexed systems are sensitive to object motion. Their multi-frame nature slows down the acquisition speed and requires the object to be stationary during the sequential projections. One approach to address this problem for the multi-frame techniques is to increase the projection/capturing rate [10] by improving the software and tuning the hardware architecture. However, this only decreases the moving effects during the projection/capturing. But the reconstructed phase remains quite sensitive to intensity noise in the captured image. The noise sources might include projector illumination noise due to fast capturing like flicker, camera noise and thus increasing synchronization requirements between projector and camera. Though multi frame techniques are accurate to obtain information of discontinuities, their long measurement procedures are time consuming making them unsuitable for detecting dynamic objects [28].

2.3 Single Pattern SLI Techniques

Single pattern techniques are focused on speeding up the acquisition process. Being able to capture shape from a single pattern opens up the possibility to use high resolution cameras whose capture rate is too slow for multi-pattern. Single pattern techniques usually employ spatial encoding algorithms with a single static projection pattern [21], where the projected patterns are encoded by spatial markings, called sub patterns. Being called as one-shot systems, they are able to extract the depth data from a single gray-level or color snapshot of the scene [15, 19] hence suitable for measurements of moving objects.

2.3.1 Composite pattern

The spatial dimension orthogonal to the dimension of depth distortion has been used effectively with the principles of simple communication theory to modulate and combine multiple patterns into a single composite pattern [15] thus making it suitable to capture moving or non-rigid data in real time. Taking advantage of the existing multiple patterns and multi-frame techniques like traditional PMP the characteristics of albedo sensitivity and non-ambiguous depth etc are preserved [9] while only projecting one single pattern onto the target object. Due to simple communication model employed the abrupt albedo variations on the edge of the circle generate space-variant blurring which results in the depth errors around the edges. These step changes containing high frequency components might cause the cross talk between the modulation channels and introduce the “wave” like artifacts and blur the depth reconstruction [16]. However, this technique suffers from low depth resolution and also carrier frequency detection in the captured pattern.

2.3.2 Multi-color techniques

Multi color - encoded techniques are one-shot measurements and hence desirable for dynamic object inspection and measurements. Stripes are generally encoded by colors and recorded using color camera sensor devices providing additional degrees of freedom to identify the stripes by arranging the colors in a distinguishable order [28].To analyze surfaces with large depth discontinuities it seems that the color-encoded projection is more practical than black and white because the unwrapping ambiguity is reduced. However the systematic precision of color-encoded techniques is generally not high enough since the measurement is highly related to the stripe width.

Kak and Boyer [20] were the first ones to design a system for acquiring the entire range map of a scene in a single grid color projection requiring only one image using color stripe indexing strategy. The projected color sequence consists of horizontally concatenated subsequences each with fixed number of vertical colored stripes. After capturing the image stripe indexing is done whenever match is detected between the n-stripe color patterns of a given subsequence with n contiguous elements of the captured pattern and stored in a list of matching correspondences. There after the range at stripe illuminated image points can be calculated by triangulation. Though the system design is inexpensive, robust and fast due to it limitation in indexed based decoding strategy not every stripe in the concatenated subsequences are uniquely identified. The sequence in which stripe reflections appear in image plane is not necessarily the same as the projected due to various factors like occlusions and surface non-uniformity etc and hence a possible ambiguity issues may arise in the identification of the stripes thus leading to inaccurate reconstruction results. Also if observed each subsequence is non ambiguous by itself but the colors are repeated in corresponding subsequences thereby ambiguity occurs in matched sequences of the received pattern. Tajima and Iwakawa [23] a rainbow 3-D camera for shape measurement which has the capability of obtaining range information for all image pixels with only one frame color camera. They used the rainbow pattern with continuous change of light color for one-shot imaging. Geng [24] improved the

rainbow pattern technique further to acquire full frame of 3-D range images from only a single image capture directly at the camera frame rate. In this technique the color of projecting light is a passed through linear variable wavelength filter as spatially continually varying wavelength light which is thereby used to generate a rainbow pattern and a CCD camera is used to capture the illuminated scene and obtains 3-D range information through active triangulation algorithm. However, since the projected pattern is composed of a continuous color spectrum, the resolution of the system is dependent on the camera's ability to distinguish among different wavelengths [27].The above proposed striped pattern projection coding along a single axis suffered matching or correspondence problem between both image planes (i.e. projector and the camera). Salvi et al [22] used a single fringe pattern with a sequence of horizontal and vertical slits to improve robustness of the matching and easy segmentation. The colored pattern used here is from a set of six different colors of HIS cone, 3 of them being used for each axes and slits have been colored with the aim that each slit with its two neighbors forms unique triplet in the whole pattern. The captured image is processed to detect segments of grey level with which colors are coded in a single image and reconstruction is achieved using image filtering and thinning technique. Segments cannot be used to detect the sharp discontinuities because cross-points are not accurately detected. Liu et al [25] demonstrated fast and efficient technique for shape measurement with a single exposure using color-coded binary grating procedure using eight colors and each color represents only one logical state. The color stripes are grouped such that each group represents the place of unit in the binary system thus providing higher grating space and positions of the stripes are stored in a reference array. In the decoding process the position of deformed stripes due to object are stored in an object array. Thus by applying arithmetic procedure on above array shift of the color stripes on the object with respect to reference plane is obtained thus calculating height information. There is couple of problems with projection grating system. The first one being correspondence (i.e. matching between the stripes on the object with the stripes on the reference plane) and other limitation occur when the minimum size of the object in the vertical direction is less than the group size (i.e. if the object area cannot hold group size, the stripes cannot be recognized). Huang et al [26] proposed a digital fringe projection technique as a little variation of traditional

phase shifting techniques by using color-encoded pattern whose RGB components comprise three phase-shifted patterns created by software to illuminate the target using DLP projections system for high image quality. To extract 3-D information the captured image is separated into individual RGB components creating three phase-shifted gray-scale images; hence by applying phase wrapping algorithms the 3-D surface contour of the target is reconstructed. Though this technique achieved high speed surface contouring it does comes with increase in cost of expensive digital projection system. Moreover measured colors are a combination of the colors of the projected fringe pattern and the colors of the object being measured. Since it is impossible to separate the combined colors without calibration, this technique is suitable only for the measurement of objects with neutral color. [27]. since the conditions for calibration are not assured to be best any measurement error may further increase if the nature of the object surface is drastically changed. All the above techniques encoded color into fringe pattern allowed for more information to be included in the same number of patterns than did the grayscale techniques. Although phase-shifting methods are effective for fringe analysis the requirement for three images to obtain phase information makes them non suitable for on-line inspection and also the noise of the CCD camera has greater influence on the measurement accuracy [27]. Although multi-color techniques can in principle produce range images with high speed and high resolution only restricted by system resolution, they are sensitive to object surface colors.

2.3.3 Lock and hold

This technique is developed to improvise the single pattern techniques to facilitate more accurate motion capture. This strategy uses the set of patterns with high resolution to lock on to the surface and then hold on to the surface deformations. If the locking phase is accurate then hold pattern does not have to be non-ambiguous. Once locked, using methods like multiple pattern PMP or boundary subdivision to determine snake identity a single pattern is projected onto the object during the “hold” phase [17]. Since it is a single pattern, the camera does not have to synchronize with it, thus the images can be captured at the video rate of the camera. The hold pattern consists of a set of stripes which we detect and track using tracking algorithms as the subject makes a series of

facial animations. Lock and Hold uses an additional pattern of snakes to track changes in the subject surface through multiple frames, allowing a phase map to be updated accordingly [18]. Due to the nature of the snake pattern, the phase map created for each frame in a sequence is not as dense as a full PMP scan. The accuracy with which correspondence between camera and projector image planes is improved using snake detection process [7]. It allows to pin-point specific projector coordinates accurately. System accuracy can be affected by the speed and direction of subject motion as well as the frame-rate of the camera being used.

Chapter 3 Color Multiplexed Single Pattern

3.1 Introduction

Optical 3D sensing techniques based on SLI methods have the properties of nondestructive detection and high depth accuracy. The proposed technique is a color-coded light via spatial encoding with a single colored projection pattern. A color image can be separated into multiple independent color “channels”; for example its red, green, and blue components. Color-multiplexing simply combines individual patterns into a single pattern by coloring each of three channels red, green and blue. In this way, each pattern can be isolated independently of the others by considering only R, G, B channel of the captured image. Hence each channel image is effectively identical to a single frame of existing multi-pattern techniques. This fact is used in 3D data acquisition in order to increase the amount of information available in a single image capture. By projecting a pattern in which each color channel contains different information and capturing the image with a high resolution digital camera, a single image can be acquired equivalent to three grayscale pattern captures. The primary aim of this chapter is to describe Color Pattern processing. First the layout of complete system with pictorial illustration is introduced. Then, each of the major algorithms used during the procedure is introduced and explained in detail.

The process of the entire system is shown in Fig. 3.1. This system consists of slide projector, a CMOS color camera and a PC. Specifically, a simple slide projector suffices to generate the necessary un-varying controlled illumination.

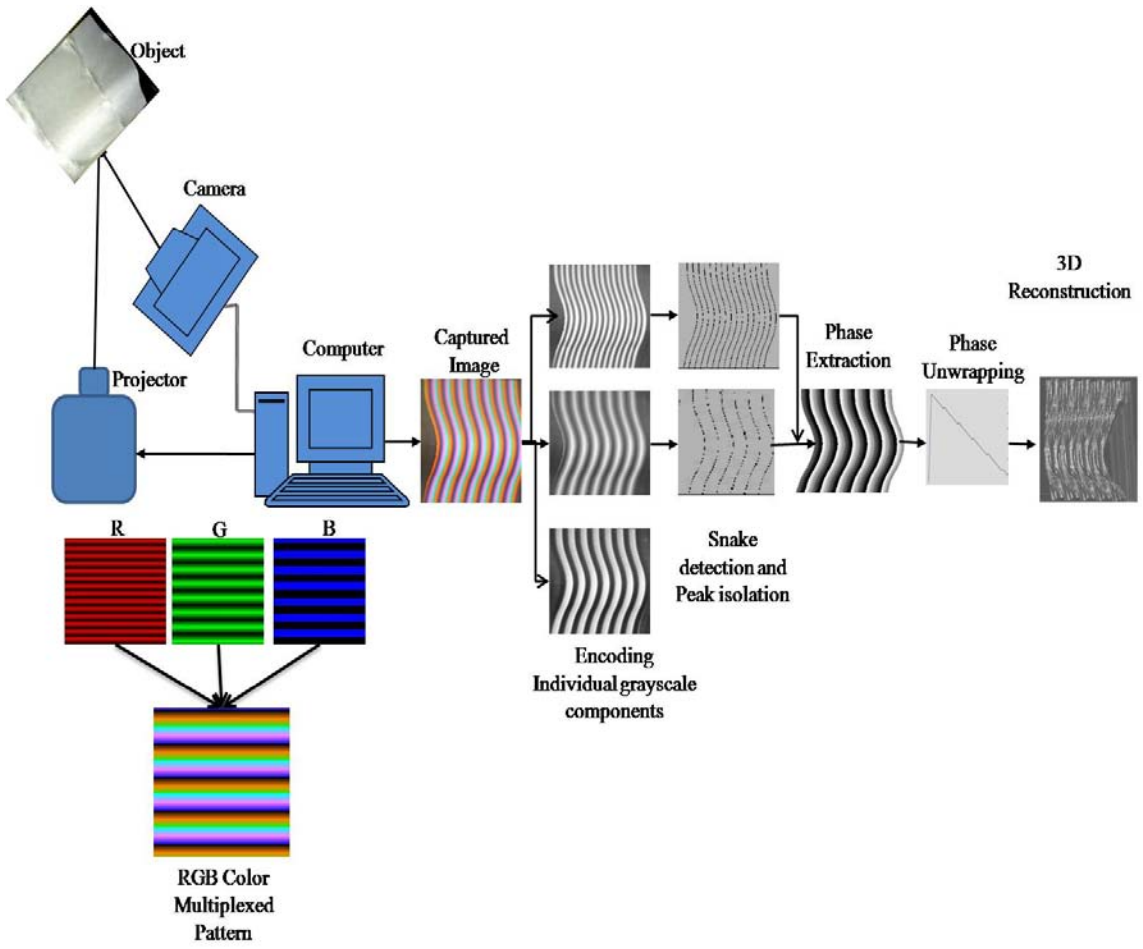

Figure 3. 1 Block diagram of the 3D acquisition system using color pattern technique

The 24-bit color pattern is encoded with unique subpatterns each of which is an 8-bit gray scale image created by software in the computer. The overall pattern is composed of a repeated subpattern of intensity values ranging from 0 to 255 in three color channels (RGB) with particular subpattern being uniquely defined for each of the channel. We illuminate the scene with a vertically striped pattern of colors from the slide projector. The reflected image of the target object is captured by the high resolution digital camera positioned at a certain angle with respect to the projector. The captured image is sent to the PC, where it is separated into its RGB components, creating three gray-scale images. For more accurate color detection, prefiltering is applied to improve the signal-to-noise ratio. These individual channel component images are then used to calculate the phase distribution distorted by the object depth and wrapped between the scale of 0 to modulo 2π. Phase extraction process uses an addition pattern of snakes to calculate the phase

value according to the surface variations in the subject. The extracted phase is used to establish a correspondence between camera and projector space. Then a phase unwrapping algorithm is used to create a non-ambiguous phase map. Using the phase map and calibration information we reconstruct the 3-D depth of the object surface.

3.2 Color Pattern Processing Algorithms

3.2.1 Pattern Generation

The parameters required to generate a 24-bit color map image are chosen according to experimental requirements. The subpattern for each channel (RGB) is generated with stripes of varying periods. Each subpattern is an 8-bit image with intensity values ranging from 0 to 255. The subpatterns are then combined into single bitmap image which is used as a projection pattern.

Step1: Design of Projection Pattern

Let the chosen dimensions for each subpattern be *MxN*, (*M* rows by *N* columns). Let K_p be the number of bands or cycles per field of view (FOV) where period T_c given as

$$T_C = M_y / K_p \tag{3.1}$$

Where *y* represents particular column index position in the bitmap image.

A 1D vector of discrete values is created as function of T_c that establishes triangular striped subpattern of varying no of cycles/period for red and green color channel and a square striped subpattern for blue channel. The subpattern for red channel is designed along the phase direction Y_p with twice the number of cycles that of green channel subpattern within the period T_c *as* given by Eq(3.2) and (3.3).

$$I_r = \begin{cases} m_1 y + 0 & for \quad 0 \le y \le T_C/2 \quad \text{and} \quad T_C/2 \le y \le 3T_C/4 \\ m_2 y + 255 & for \quad T_C/2 \le y \le T_C \quad \text{and} \quad 3T_C/4 \le y \le T_C \end{cases} \tag{3.2}$$

$$\begin{aligned} m_1 &= 255/(T_C/4) \\ m2 &= -255/(T_C/4) \end{aligned} \tag{3.3}$$

Where m_1 and m_2 are the slope of intensity variation calculated as a function of period T_c. The subpattern for green channel is designed along the phase direction Y_p with half the number of cycles of the red channel subpattern within the period T_c as given by Eq(3.4) and (3.5).

$$Ig = \begin{cases} m_1 y + 0 & \text{for} \quad 0 \le y \le T_C / 2 \\ m_2 y + 255 & \text{for} \quad T_C / 2 \le y \le T_C \end{cases} \tag{3.4}$$

$$\begin{aligned} m_1 &= 255/(T_C / 2) \\ m2 &= -255/(T_C / 2) \end{aligned} \tag{3.5}$$

And blue channel subpattern consists of an intensity value 0 for half the period T_c followed by intensity value 255 for remaining half of the period as given by Eq (3.6).

$$Ib = \begin{cases} 0 & \text{for} \quad 0 \le y \le T_C / 2 \\ 255 & \text{for} \quad T_C / 2 \le y \le T_C \end{cases} \tag{3.6}$$

Where y represents the column position in the image, I_r ,I_g and I_b are the intensity values for each position of y. This function has to be repeated K_p times across the image for each row in the orthogonal direction across the image.

Fig 3.2 depicts individual color channel components with stripes of varying width designed according to their respective equation.

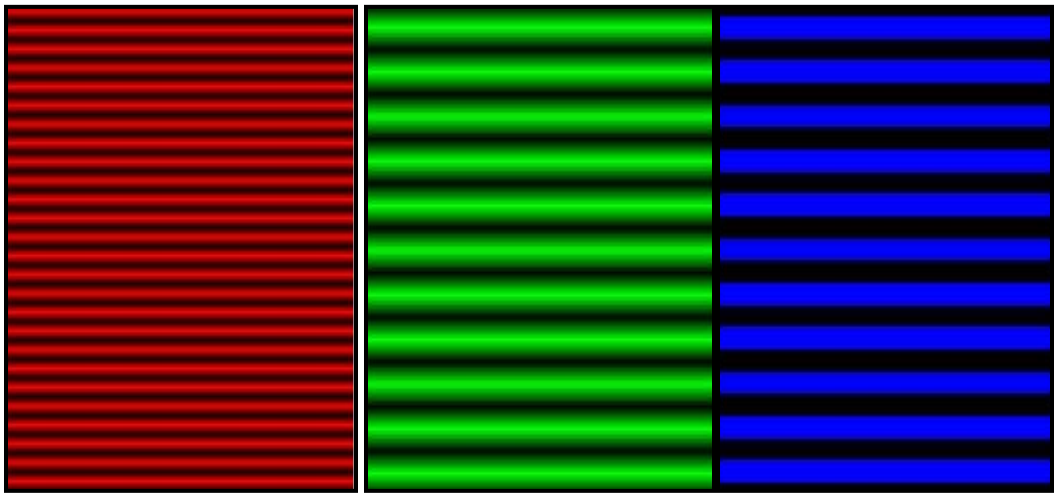

Figure 3. 2 R,G,B subpatterns

These subpatterns defined uniquely for red, green and blue channel are combined to form 24-bit color bitmap image. The projection pattern used in this work has resolution of 1200x1800 with 32 cycles per field of view as shown in Fig 3.3.

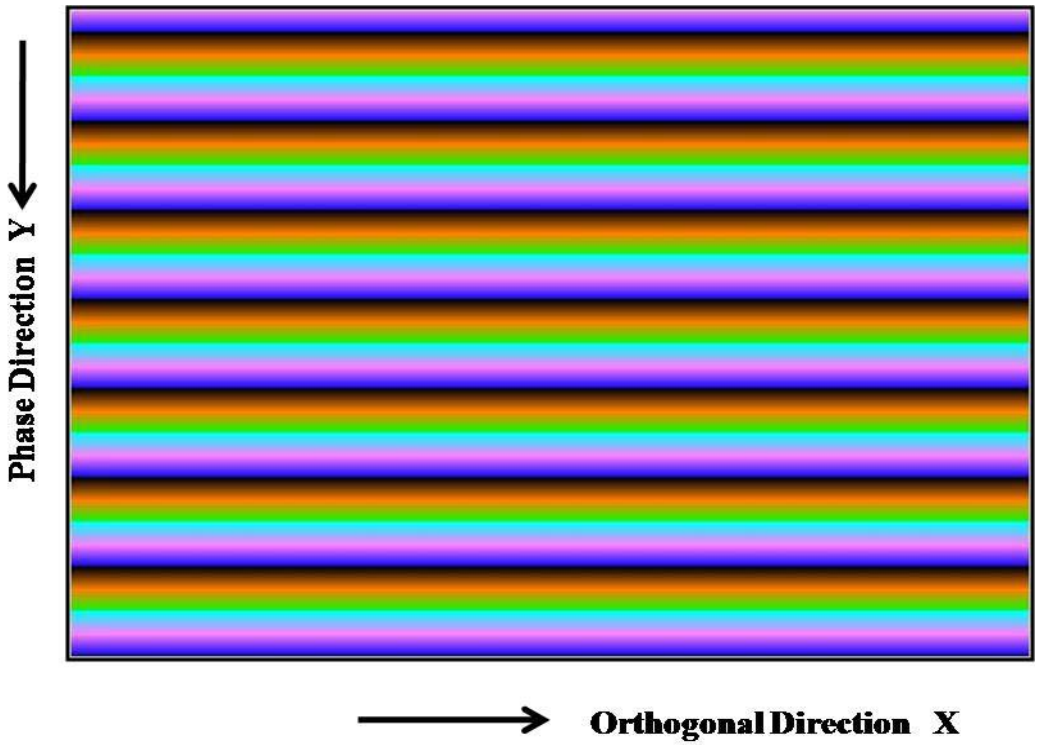

Figure 3. 3 RGB color multiplexed pattern

The cross-section graph shown in the Fig 3.4 is obtained by plotting across one specific column of the projection image in Fig 3.3.

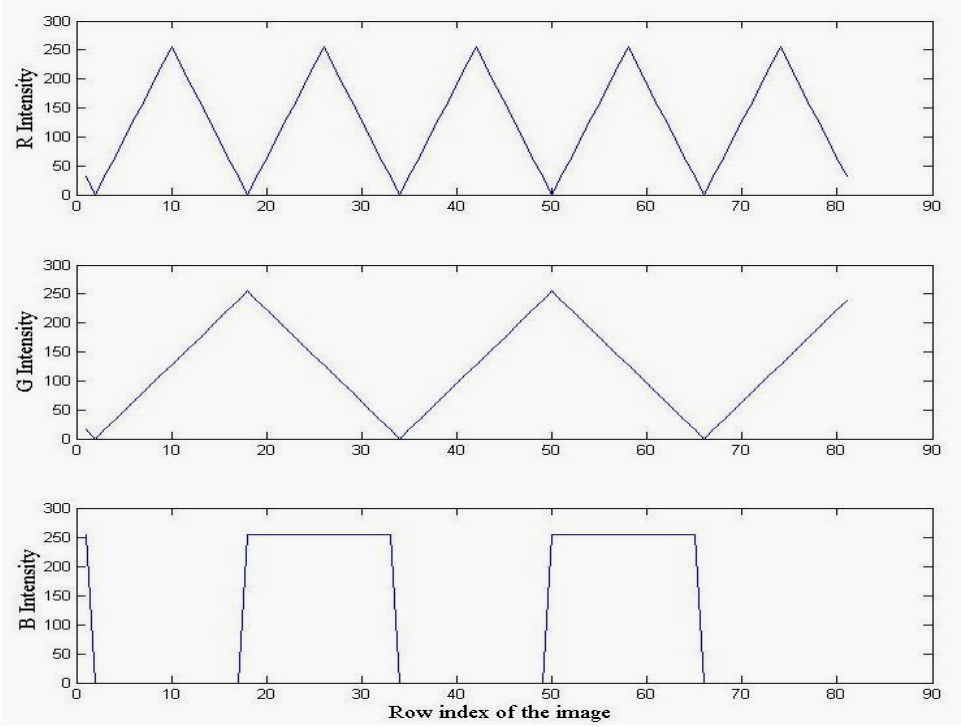

Figure 3. 4 Ideal Cross-Section of SubPattern in individual channels (R, G, B)

The upper subplot refers to Red channel triangular cross-section which indicates the period twice to that of middle subplot of Green channel component and their intensity levels varying from 0 to 255 .The lower subplot refers to blue channel component which has two intensity levels 0 or 255.

3.2.2 Decoding

Step2: Seperating RGB color captured image into individual channels

Fig 3.5 shows the scan of the object captured by projecting the color multiplexed pattern. As shown the phase direction is changing according to the surface variations of the target object.

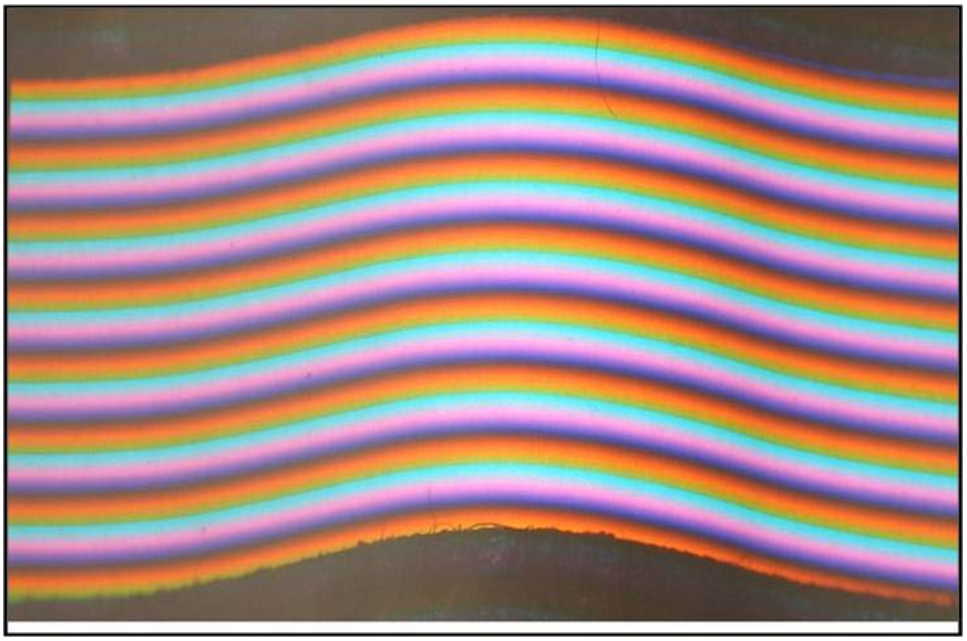

Figure 3. 5 Cosine manifold image with color multiplexed projection pattern

Let *C* be the captured image of the subject. Read the color captured image and separate it into R, G and B components. Let C_i corresponds to each grayscale component images in Red, Green and Blue channels respectively. The individual component images are prefiltered to remove the noise. Pre-filtering the encoded image is done using a moving average window - i.e. a 3x1 column filter; given by F= [1/3; 1/3; 1/3]. The regularization properties of the filter guarantee the continuity of the derivatives of the smoothed image. The individual monochromatic component images in each channel are processed for

snake detection and peak isolation. This snaking process is done using an algorithm that performs a pixel-based intensity analysis of the input image. By performing snake detection, we can locate the peaks in the image and thus make it easier to unwrap the phase image.

3.2.3 Snake detection and peak isolation

A snake can be visualized as a single pixel thick stripe created by processing the image of an object illuminated by the projection pattern [7, 18, 32]**.** The projection pattern modification used in our methodology consists of a field of stripes (or "snakes") which are triangular, with intensity values along the snake ranging from 0 to 255 as per design without loss of generality (and is the source of the identifier "snake"). The stripes in the snake matrix corresponds to the illuminated light bands due to R, G, B component images in the captured image pattern. Snake matrix of individual component images is used to decode the phase value to be used for 3D reconstruction. In our system snake peak isolation is done via peak-to-side-lobe measurements. The PSR is albedo invariant because it is a ratio, thereby canceling the multiplicative factors of albedo and reflected light.

Step3: Finding the peak to side lobe ratio

For each monochromatic component image C_i, a temporary image of same size is created to contain the peak-to-side- lobe ratio (PSR) measure at each point in the corresponding input image. There are two approaches to the PSR. One is based on a linear acquisition of the sidelobe intensities and the other is an ordered based approach. For the linear approach the PSR is determined as the ratio of the square of the peak divided by the square of the sidelobe value. Because we are using the technique for accurate peak isolation, it is numerically more efficient to use the non-squared version i.e ordered. The ordered *PSR* represents the worst case scenario by using the greater of the two sidelobes.

For each pixel two pixel locations on the triangular cross-section around the pixel under consideration are collected and side lobe value is assigned as maximum value among those two pixels [18].

$$Sidelobe = \quad Max(C_i[x, y - Pd], C_i[x, y + Pd]) \tag{3.7}$$

Where P_d is predefined sidelobe offset value. Next the PSR value is obtained by the Eq(3.8)

$$PSR[x, y] = \quad \frac{C_i[x, y]}{Sidelobe} \tag{3.8}$$

Step4: Finding the Positive Snakes:

Positive snake represent the pixels of the snake which has the maximum intensity value in the individual channel grayscale components of the captured image and termed as "positive peaks". With the high signal-to-noise ratio positive peaks improve measurement accuracy. Positive snake peaks detection is performed by looking at the locations where *PSR* is maximum as snakes represent the maximum *PSR* locations. Let $\underline{S_p}$ be the 2D snake image of integer values. Every snake represents a row in the snake matrix. The PSR image obtained in the above section is thresholded using a user defined minimum PSR value *(PSR_{min})* and the intensity or the peak value at that pixel must be greater than a predetermined minimum value ($PEAK_{min}$).

$$PSR_1[x, y] = \begin{cases} PSR[x, y] \text{ for } PSR[x, y] \geq PSR_{\min} \text{ and } C_i[x, y] \geq PEAK_{\min} \\ 0 \quad \text{otherwise} \end{cases} \tag{3.9}$$

Step5: Peak isolation

Within each column of the input component image C_i a vertical search is performed until an subsection is found which may contain a snake peak location, that is, a region of PSR_1within a vertical range *y-i to y+j* defined such that

$$\begin{aligned} &PSR_1[x, y + s] > 0 \text{ where } s \in \{-i, -i + 1, \ldots j - 1, j\} \\ &\text{and } PSR_1[x, y - i + 1] = 0 \text{ and } PSR_1[x, y + j + 1] = 0 \end{aligned} \tag{3.10}$$

Within this region, a search is again performed for the maximum PSR value. At the corresponding position of this maximum value, a peak is placed in the snake image S_p. A value of 0 in the S_p matrix signifies the absence of a valid peak, while a value of greater than 0 signifies that a valid peak is detected. The resulting regions encoded with value 1

that contains the positive snake peaks where PSR value of input image is locally maximized and every other pixel is 0.

$$S_p[x,y] = \begin{cases} 1 \; if \; PSR_1[x,y] = Max[PSR_1[x,y+s]] \text{ where } s \in \{-i,-i+1.....j-1,j\} \\ 0 \quad \text{otherwise} \end{cases} \tag{3.11}$$

Step6: Finding the Negative Snakes

Negative snake represent the pixels of the snake which has the minimum intensity value in the individual channel grayscale components of the captured image and termed as "negative peaks". Negative peaks are found by searching between two successive positive peaks of a snake across the image. The algorithm loops through the positive snake matrix S_p row elements, first checking the positive snake peak locations in the rows above and below. It stores two consecutive positive peak locations $S_p[x,y_1]$ and $S_p[x,y_2]$ where $y_1<y<y_2$. To get the negative peak location within this range a vertical search is made in the input component image C_i between the upper and lower positive snakes which enclose the negative snake pixel in question. It considers the intensity value of each pixel according to the following equation (3.12) and encodes S_n matrix with value 1 as negative snake location in according to the position of the minimum intensity value in the input image given by.

$$\begin{aligned} &S_n[x,y] = 1 \text{ if } \quad C_i[x,y] = Min\{C_i[x,y+s]\} \quad \text{where } s \in \{-i,-i+1.....j-1,j\} \\ &and \; S_p[x,y-i+1] = 1 \; and \; S_p[x,y+j+1] = 1 \end{aligned} \tag{3.12}$$

3.2.4 Phase Decoding

Phase extraction step is used to decode the phase of input image to be linear to get non-ambiguous range. The snake matrix in Red and Green channel is used to decode the non-ambiguous phase value by defining independent subsections. The subsection for phase extraction processing that is obtained from positive and negative snake matrices between consecutive negative peak locations in the green channel as shown in Fig 3.6.The same subsection is repeated over entire image in each channel. The phase for each column of the image must be linear between same initial and final value. The phase-extraction leads to phase-wrapped image with the highest gray level corresponding to phase of 2π and the lowest to 0.

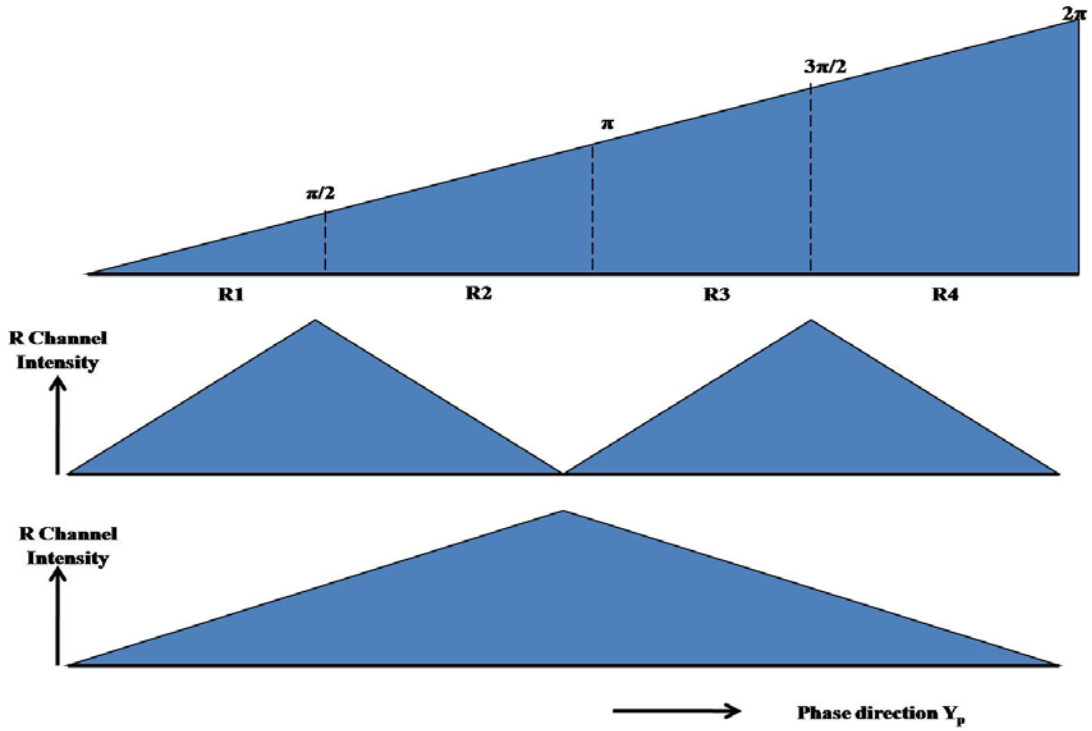

Figure 3. 6 Cross-section region of the image for Phase calculation

Fig 3.7 illustrates a section of one of the 8-bit gray scale component image. The theoretical intensity value at any point between consecutive peaks is obtained by the Eq 3.13.

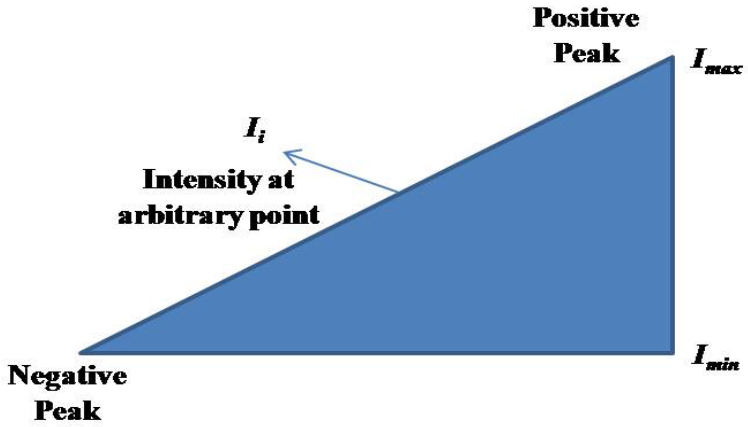

Figure 3. 7 Cross-section of 8-bit gray scale component image

$$I_{out} = (a * I_i) + b \quad \text{where } (a * I_{\max}) + b = 255 \text{ and } (a * I_{\min}) + b = 0 \tag{3.13}$$

Where I_i is current pixel position, I_{max} is positive peak location, I_{min} is negative peak location in the image. The above theoretical intensity values are used to determine which region the subsection of gray scale image belongs to and the appropriate linear interpolation equation is applied to calculate the phase between 0 and 2π.

Let R_i and G_i are the normalized intensity values between 0 and 255 for the pixel under consideration. R_s and G_s contain slope values between a consecutive positive and negative peak of red and green channel respectively. The normalization is done using positive and negative peaks of respective channels given by d_1 and d_2.They are used to define the boundaries of the regions to calculate the phase value.

P_{01} gives the phase value for the pattern sub regions R_1 where $R_s>0$ and $G_s>0$.

$$P_{01} = \left(Ri + (2 \times Gi) \middle/ (d1 + d2)\right) \times \left(\pi \middle/ 2\right) \tag{3.14}$$

P_{12} gives the phase value for the pattern sub regions R_2 where $R_s<0$ and $G_s>0$.

$$P_{12} = \left(((d1 - Ri) + (2 * (Gi - d2/2))) \middle/ (d1 + d2)\right) \times \left(\pi \middle/ 2\right) + \pi \middle/ 2 \tag{3.15}$$

P_{23} gives the phase value for the pattern sub regions R_3 where $R_s>0$ and $G_s<0$.

$$P_{23} = \left((Ri + (2 * (d2 - Gi))) \middle/ (d1 + d2)\right) \times \left(\pi \middle/ 2\right) + \pi \tag{3.16}$$

P_{34} gives the phase value for the pattern sub regions R_4 where $R_s<0$ and $G_s<0$.

$$P_{34} = ((d1 - Ri) + (2 * (d2/2 - Gi))) \middle/ (d1 + d2) \times \left(\pi \middle/ 2\right) + 3\pi \middle/ 2 \tag{3.17}$$

3.3.5 Phase Unwrapping

In our proposed method phase unwrapping algorithm assigns a non-ambiguous value for every pixel of the image on the scale of modulo 2π. For every pixel on the offset image the value is equal to the number of snakes corresponding to the phase value of 2π which are above the point in the offset image.

$$O[x,y]=\sum_{i=0}^{x} R_4[i,y]+1 \quad \text{where } R_4[x,y]=1 \text{ if } R_n[x,y]=1 \text{ and } G_n[x,y]=1 \tag{3.18}$$

The unwrapped phase image is created by multiplying the offset image by 2π and adding it to the original phase image at each point. Since the unwrapped phase map has to be between 0 and 2π the normalization is applied to unwrapped phase image. Find the maximum value of phase in unwrapped image and divide the entire image using that value. Finally multiplying resulting image with 2π gives the unwrapped phase image between 0 and 2π.

3.3.6 Summary of color pattern processing

The pattern generation algorithm gives mathematical analysis of color-multiplexed pattern. From the captured image, one must isolate three gray scale information images of each color channel. The Decoding process does this separation and applies filtering technique to ensure the noise is reduced before further processing. Snake tracking algorithms detect and isolating positive and negative peak intensity pixels of individual channels. Phase extraction algorithm uses the information in the snake images to define the boundary conditions for a phase calculation across a single column. The phase pixels present are then extended across the whole image using the snake image. Finally phase unwrapping algorithm combines this phase image with the offset image created using snake image, to get unwrapped phase in which each pixel of the captured image is assigned a unique value on the scale of 0 to 2π thus creating corresponding with the pixel of the projected image. This image can be used directly along with calibration information to calculate the world coordinates of the surface. Various steps of color pattern processing are illustrated through flow chart in Fig 3.8

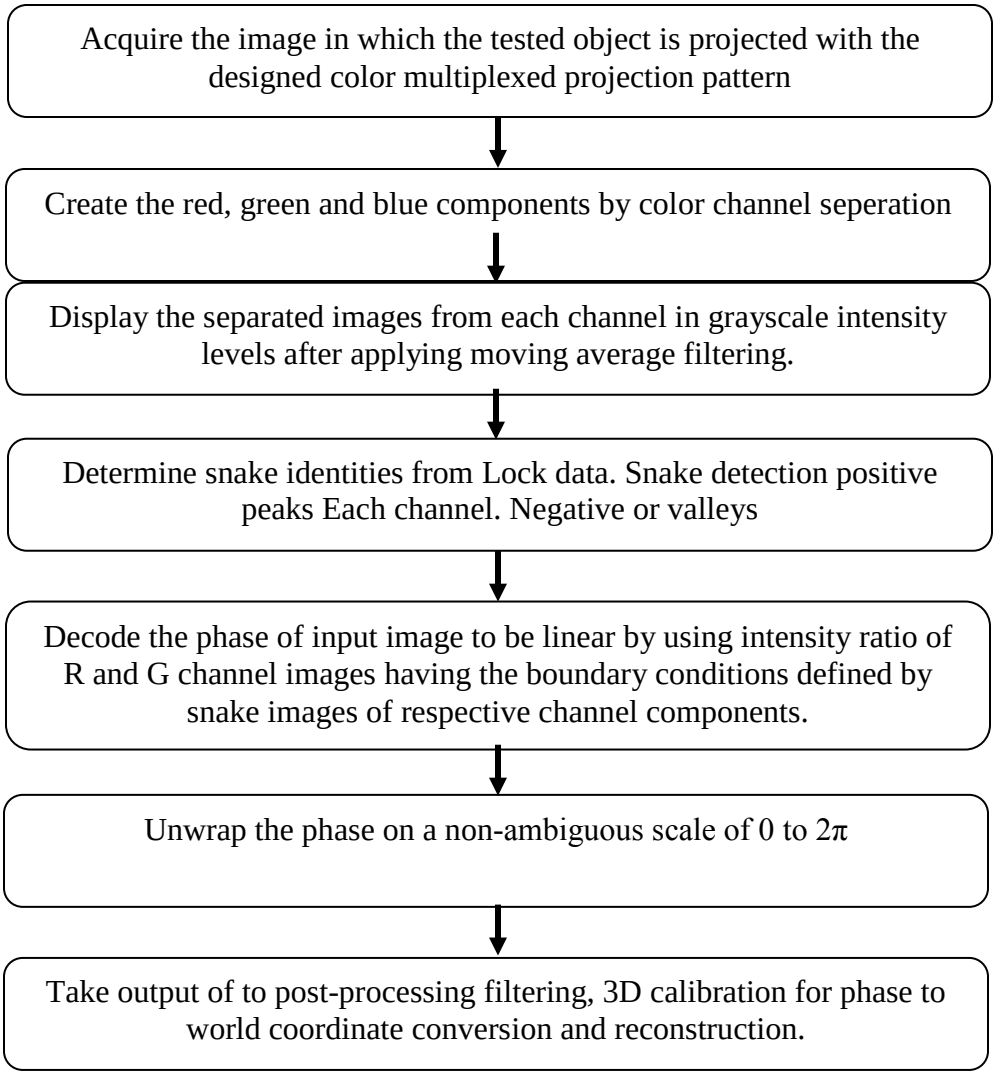

Figure 3. 8 Summary of color pattern processing

3.3 Calibration Procedure

Calibration is an important step in 3D computer vision in order to extract depth information from the 2D images. It allows the phase image to be mapped to a surface in world coordinates. In the calibration for the SLI system, both the camera and the projector need to be calibrated. It involves the transformation of the three coordinates represented as 3D Euclidean space X_w, Y_w, Z_w which are measured in metric units, the camera coordinates represented as X_c, Y_c measured in pixels and the projector coordinates as, Y_p measured in pixels or Y_p the phase dimension in radian units.

The Fig 3.9 illustrates the experimental setup used for calibration procedure.

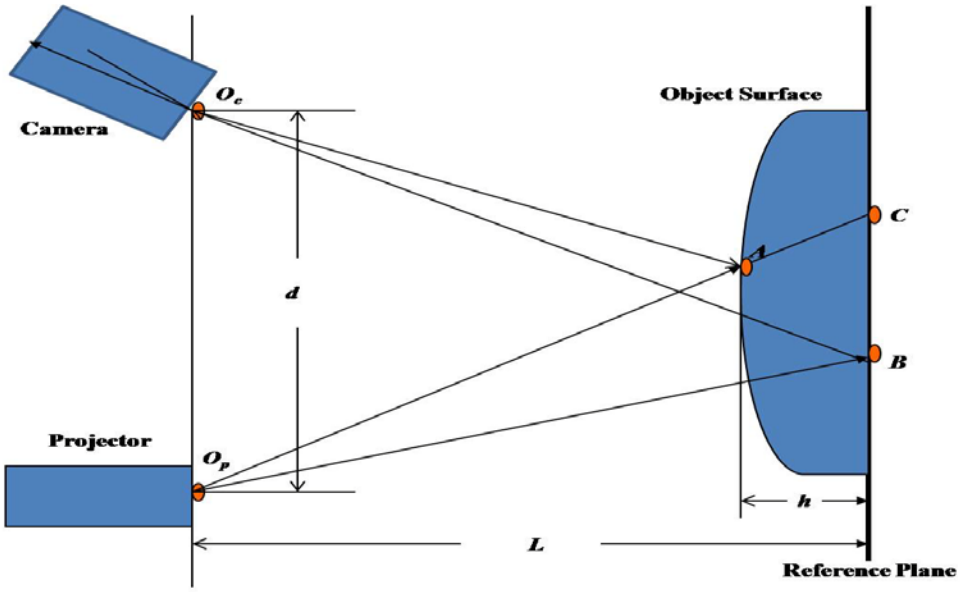

Figure 3. 9 Calibration setup to measure height *'h'* of the object surface [28]

The distance between the projector lens centers O_p to the camera lens center O_c is d. Both the projector and the projector-camera plane are at a distance L from the reference plane [28, 29]. The height of the object at point A, i.e, h is calculated by

$$h = \frac{BC.(L/d)}{1+(BC/d)} \tag{3.19}$$

Where BC is proportional to the difference between the phase at point B, i.e. φ_B and the phase at point C i.e. φ_C as given by the Eq (3.20).

$$BC = \beta(\phi_C - \phi_B) \tag{3.20}$$

The geometric parameters L and d are determined during the calibration procedure. The constant β is calculated by shifting the initial reference plane position by a known distance Δh, as shown in the Fig 3.10

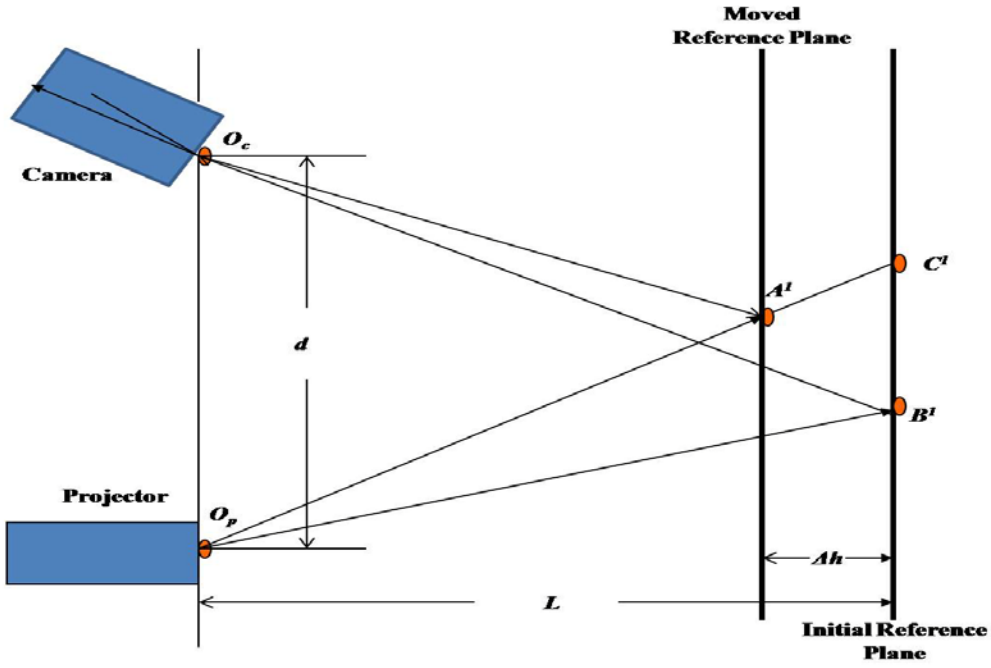

Figure 3. 10 Calibration setup to measure value 'β'

Fig 3.10 shows the experimental setup arrangement to measure the phase difference introduced by varying the initial reference plane position by a known distance Δh. The value of the geometric parameter β is calculated by the Eqs (3.21) and (3.22) respectively.

$$\Delta\phi = (\phi_C' - \phi_B') \tag{3.21}$$

$$\beta = \frac{\Delta h \times d}{(\Delta\phi)[L - \Delta h]} \tag{3.22}$$

Thus the value β is substituted in Eq (3.20) to obtain BC proportional to phase difference between initial reference plane position and object being measured and finally height of the object surface is calculated using Eq (3.19).

Chapter 4 Experiments and Results

In this chapter, the color multiplexing technique is thoroughly investigated and the experimental results are presented. The errors occurred due to various factors during implementation and experimentation part are illustrated and compared with respect to corrected and improved results. The major goal of this thesis as stated earlier is to process and analyze the captured image using a color multiplexed pattern that can be used to reconstruct the 3D data without any ambiguities. In order to test the color multiplexed pattern algorithm, a plain smooth surface and cosine manifold models are chosen as the target objects. The geometric calibration technique used is simple owing to the computational simplicity still providing accurate results. The error in 3D reconstruction due to the calibration inaccuracies also play an important role in determining the reconstruction of topology and depth information. These inaccuracies are analyzed and corrected to obtain better results.

4.1 Experimental Setup

This section illustrates the apparatus and setup used to project the pattern on the target objects. As shown in the snapshot of experimental setup in Fig 4.1 a simple slide projector is used to project the pattern and control illumination for the projection pattern The Kodak Ektagraphic IIIA projector, with auto focus option automatically focuses each slide after you focus your first slide manually. The projector lens is chosen with shorter focal length (i.e., the smaller the f/number), to get brighter projected image. To obtain the better results of a projected image, insert slides with the emulsion side toward the projection lens, slide curve toward the light source.

Figure 4. 1 Experimental setup showing hardware equipment

The canon powershot G5's 5.0 megapixel CMOS camera is used to perform the image capture. The reduction of pixel size necessary to achieve a 5.0 Megapixel CMOS calls for extremely high levels of lens performance. An optical neutral density (ND) filter is built into the lens to reduce light by 3 stops, permitting creative slow shutter versus large aperture settings in bright conditions. Various shooting modes like manual, auto and program are available.

4.2 Results of color pattern technique

This section illustrates implementation of color pattern algorithm. Errors encountered in the process and corrections made to improve them are discussed with respective graphs. The figures are arranged according to the processing steps of algorithm explained in chapter 3. Fig 4.2 is a 24-bit color multiplexed image with three 8-bit depth color channels (R, G and B) each having a unique sub patterns. The color pattern is generated in computer for projecting on to the target surface. The slide image resolution is 1200x1800 with 32 cycles per field of view.

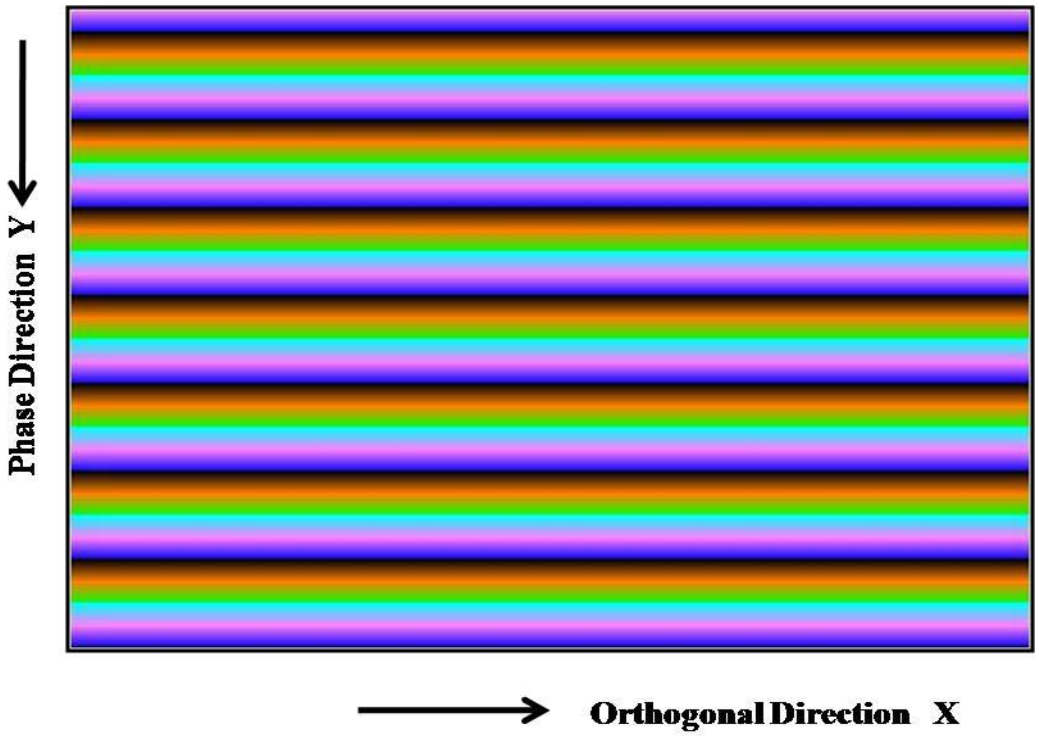

Figure 4. 2 Image of color projection pattern RGB.bmp

The cross-section in the Fig 4.3 is obtained by plotting the cross-section of projected pattern.

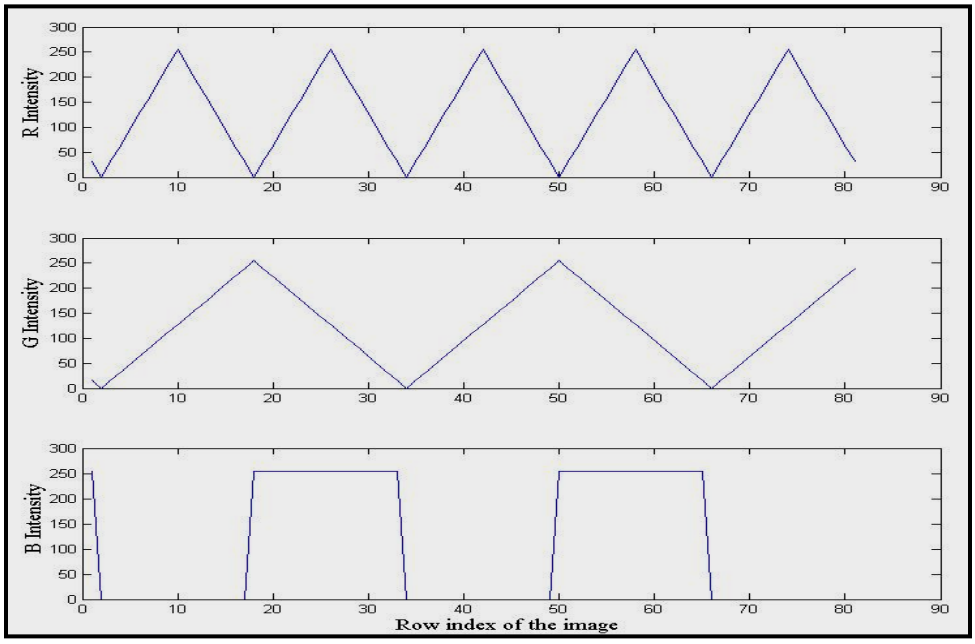

Figure 4. 3 cross sectional intensities of RGB components of figure 4.2

The upper subplot refers to Red channel subpattern with triangular cross-section and twice the frequency to that of second subplot illustrating Green channel subpattern with

their intensity levels varying from 0 to 255. Thus Red and Green channel components constitute 8-bits of useful information respectively. The lower subplot refers to blue channel component which has two intensity levels 0 or 255 thus representing 1-bit of information. The period T_c is given by equation 3.1.

4.2.1 Inter channel color interference

During the initial phase of experimentation a flat smooth surface is used as the target surface and a digital projector was used for projecting the pattern. But it is observed that due to inherent limitations of color filters of the projector and screen door effects the color wavelengths of R, G, B components there is significant inter-color interference. Due to this the inter-color interference problem nonlinearity is observed in the individual grayscale channel components (R, G, B) of the captured image. Hence we replaced the digital projector with a slide projector. Using slides which are printed with direct correspondence to bitmap RGB reduced the inter color interference to greater extent. Fig 4.4 shows an example of a scan of flat surface produced by a 5 Megapixel Canon powershot G5, using both digital and a slide projector respectively.

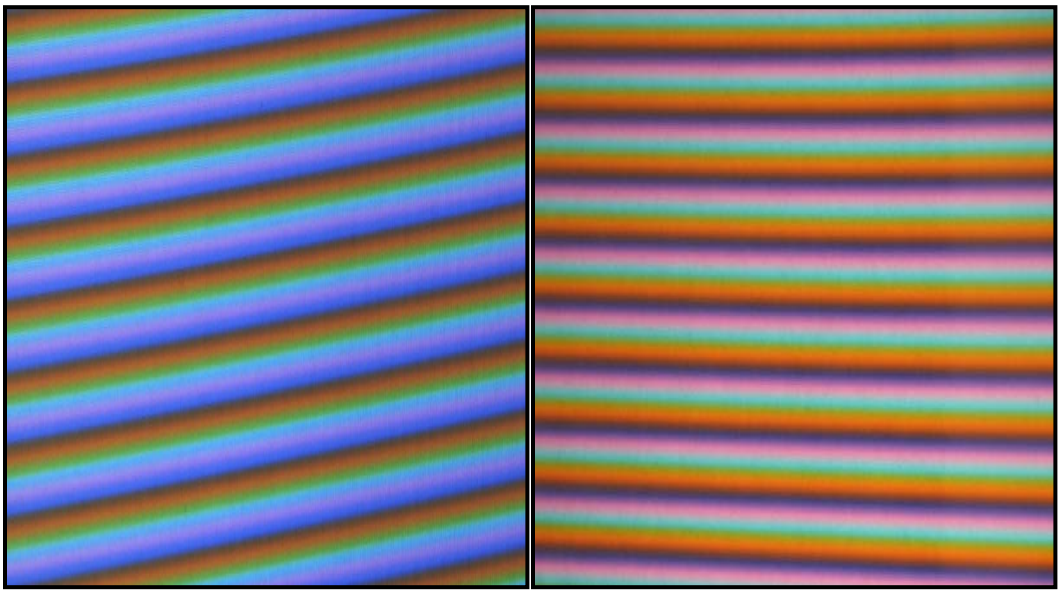

Figure 4. 4Image of captured object (Flat surface) using (a) Digital (b) Slide projector respectively

To understand the effect of inter-color interference the cross-section across a column is the three color channels of Fig 4.5 are considered. As shown in Fig 4.5a the red channel subpattern information is corrupted and the intensity variation of successive cycles is not uniform. The green channel subpattern information has non linearity and misalignment in period from other channel components. Even after filtering the errors propagated in post-processing stages and the unwrapped phase is found not accurate spoiling calculation for many pixels. Using the slide projector the inter-color interference has been reduced to a greater extent and better alignment of the subpattern in individual channels with uniform intensity variation is obtained as shown in F 4.5b.This resulted in the improvement of unwrapped phase.

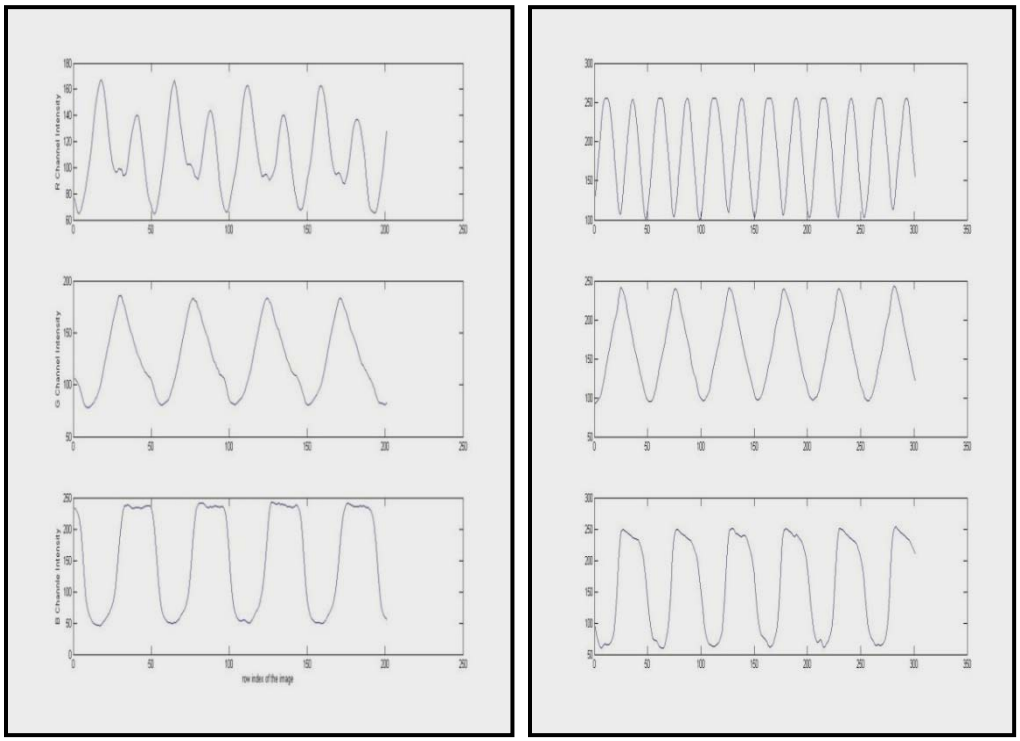

Figure 4. 5 (a) (b) Plots showing cross sectional intensities of RGB components of capture image with Digital and Slide projector , respectively.

The Fig 4.6 a through c are the cropped images of grayscale components in the RGB channels of captured image. They are pre-filtered by a simple moving average FIR filter with order 3 which regards each data point in the data window to be equally important when calculating the average (filtered) value thus reducing any random noise.

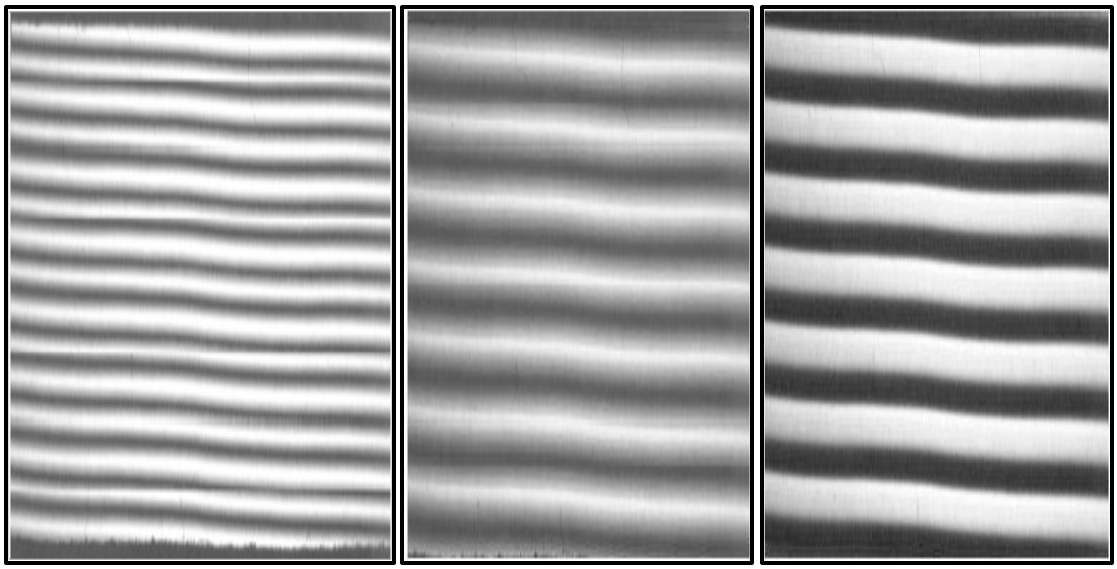

Figure 4. 6 (a) (b) (c) Encoded R, G, B channel gray-scale component images

The subpatterns of each channel are designed such that the red and green channels have the required information for calculating phase and obtaining unambiguous phase map of the image. Hence blue channel is not used in further processing stages of the algorithm.

4.2.2 Snake detection and processing

Snake detection and peak isolation is an important step for reconstruction of 3D model. Since, each peak corresponds to a single coordinate value along a dimension in projector space. However, due to noise and other surface anomalies there is a possibility of pixels being incorrectly identified as snakes. To avoid this snake detection in our method uses various isolation parameters like search range (P_d), Peak-to-side-lobe ratio (PSR_{min}) and minimum intensity ($peak_{min}$). At the same time due to the range of intensity values across the snakes, they will be sensitive to the variation in isolation parameters. This section details experiments done with variation of isolation parameters and effects observed in the detection and isolation of peaks along the snake. This analysis is based on the idea that errors frequently start as very small segments of incorrectly identified snake pixels. Therefore, eliminating these false peaks can help prevent error propagation through future processing steps.

The maximum intensity value of the snake is termed the positive peak and minimum intensity value of the snake is termed the negative peak. This terminology is used in the following explanation and figures. As mentioned in color pattern processing, the peak-to-sidelobe ratio (PSR) is used to identify the positive peak locations of the component images. Since the search range parameter P_d determines the placement of a sidelobe for calculating the PSR measure; P_d has to be chosen such that PSR is defined properly for all the snakes. Too low or too high values of P_d will cause search range to be improperly defined, reducing the number of isolated snake pixels significantly. This is illustrated in Fig 4.7 by the cross-section along a column of the captured image. The missing green spikes in the image indicate the error introduced due to improper setting of P_d.

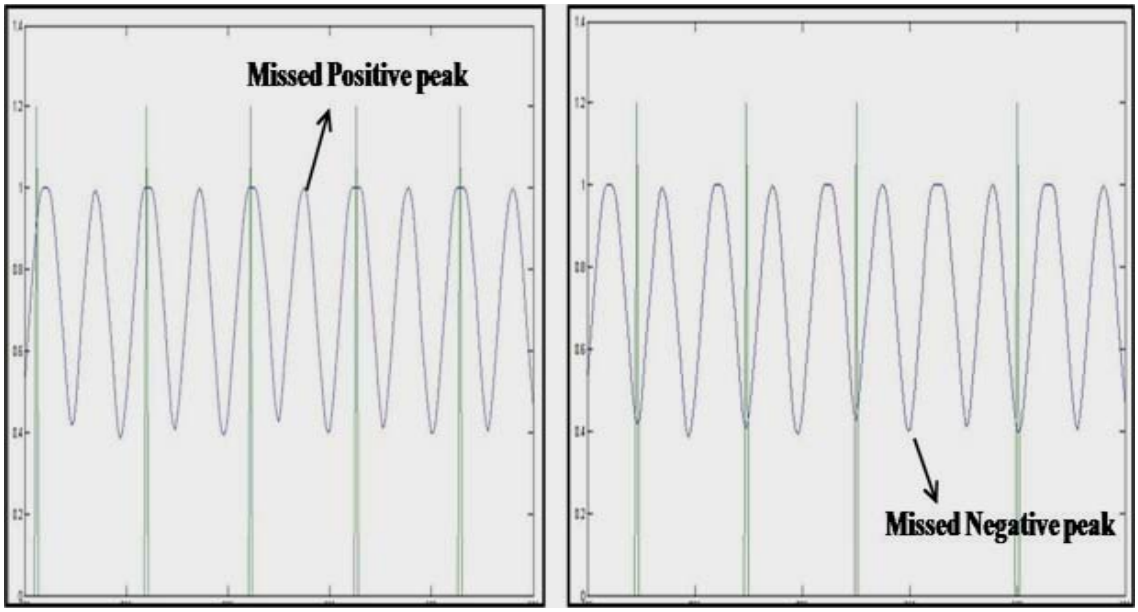

Figure 4. 7 Isolated snake peaks in R chl before proper P_d setting

Fig 4.8 shows the PSR overlapped on red channel grayscale image plotted for different values of P_d while keeping other parameters PSR_{min} and $Peak_{min}$ constant. The blue and green colored areas indicate PSR ratio from too high or too low values of P_d. In both the cases PSR is not defined properly for all the peaks of the input image, whereas the red colored areas indicate a PSR defined for all the peaks due to a proper setting of P_d.

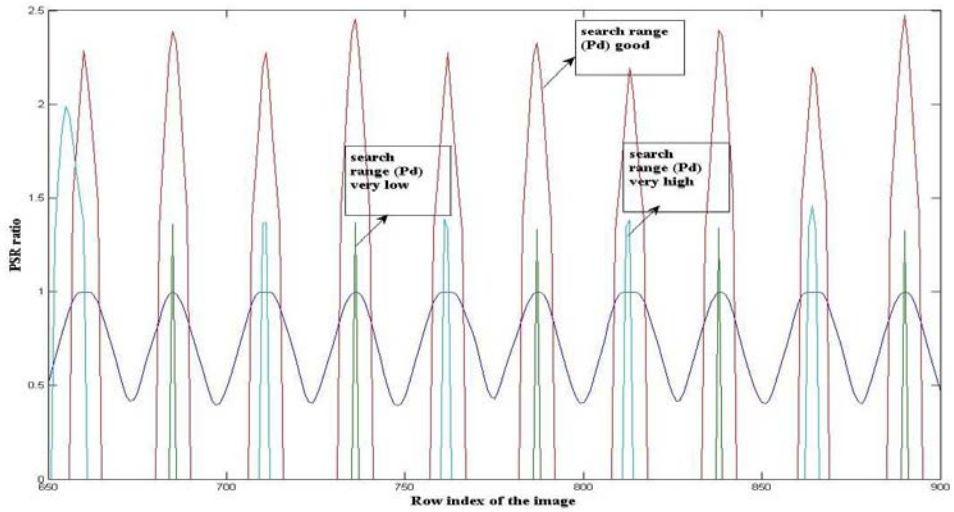

Figure 4. 8 variation of PSR with different values of Pd

By thorough analysis the reasonable good range of values for search range P_d to isolate positive peaks more accurately is given by equation 4.1

$$Pd < Px1 - Px2 \tag{4.1}$$

Since the negative peaks are searched with respect to positive peaks that surround them, and negative peaks

$$Px1 + Px2 \le Pd \le 2 \times (Px1 + Px2) \tag{4.2}$$

Where Px_1 and Px_2 is the distance between any two successive positive peaks in a single column.

Noteworthy results from experiments indicate that applying a proper threshold value PSR_{min} on the PSR ratio matrix helps to assure correct identification of the peaks. Fig 4.9 indicates how very high values of PSRmin would cut off valid PSR ratio pixels. Since the peak isolation is based on PSR ratio values this will result in elimination of valid snake pixels.

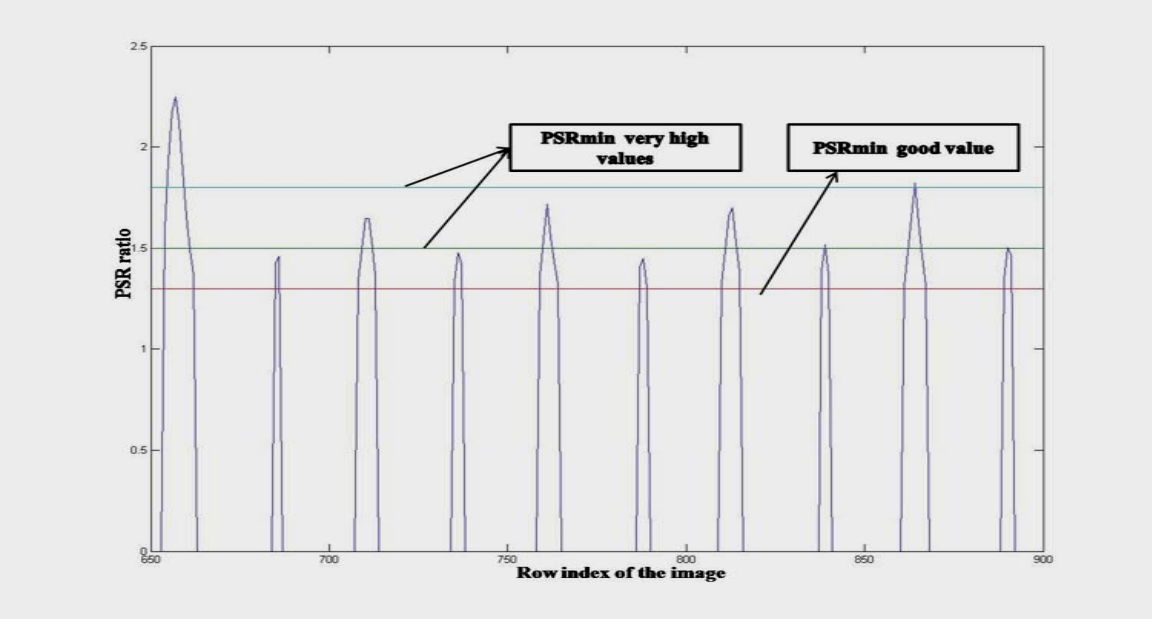

Figure 4. 9 Effect on PSR ratio with different values of PSR_{min}

The corresponding effect of improper choice of PSR_{min} is shown in Fig 4.10a where many snakes are missed when compared to Fig 4.10b with good PSR_{min}.

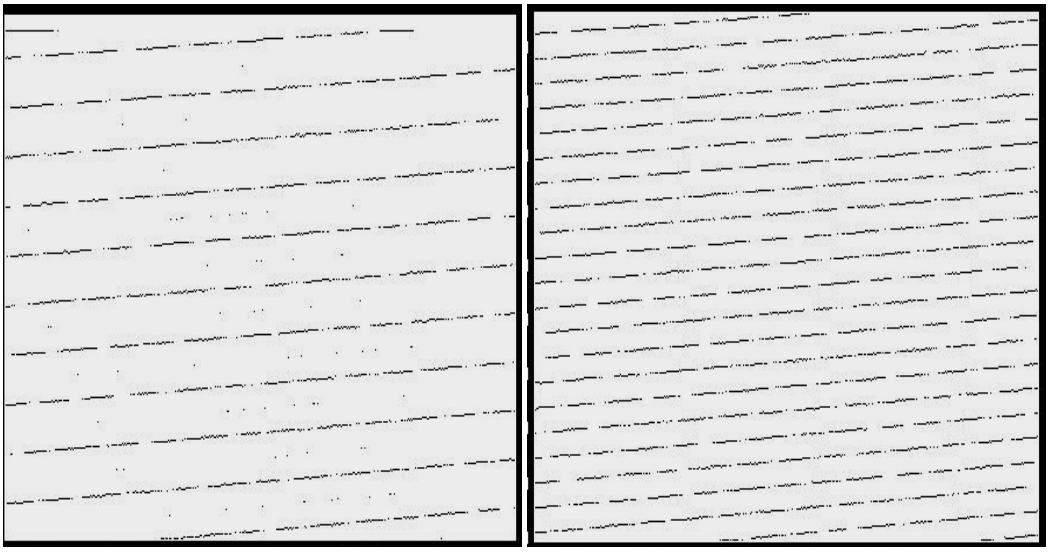

Figure 4. 10 Comparison of isolated positive snakes in R channel with (a) improper (b) Proper PSR_{min} setting

The PSR is largely albedo invariant because it is a ratio, thereby canceling the multiplicative factors of albedo and reflected light. Hence proper setting of P_d and PSR_{min} ensures proper detection of peaks and forms good snakes across the image. This effect is clearly noticed in figure 4.11 as shown by the peaks lined up accurately with the PSR cross-section indicated by blue color in the plot.

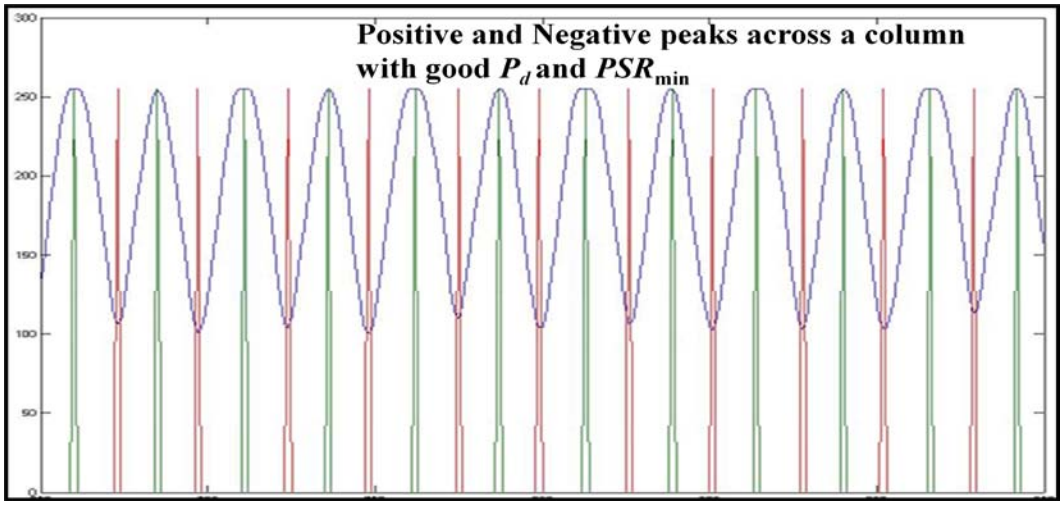

Figure 4. 11 Isolated peaks in R channel with proper P_d *and* PSR_{min} setting

When the $peak_{min}$ is too low extremities are caused by allowing false peaks due to noise being detected and seen forming misleading snakes in the image as shown in the Fig4.11.

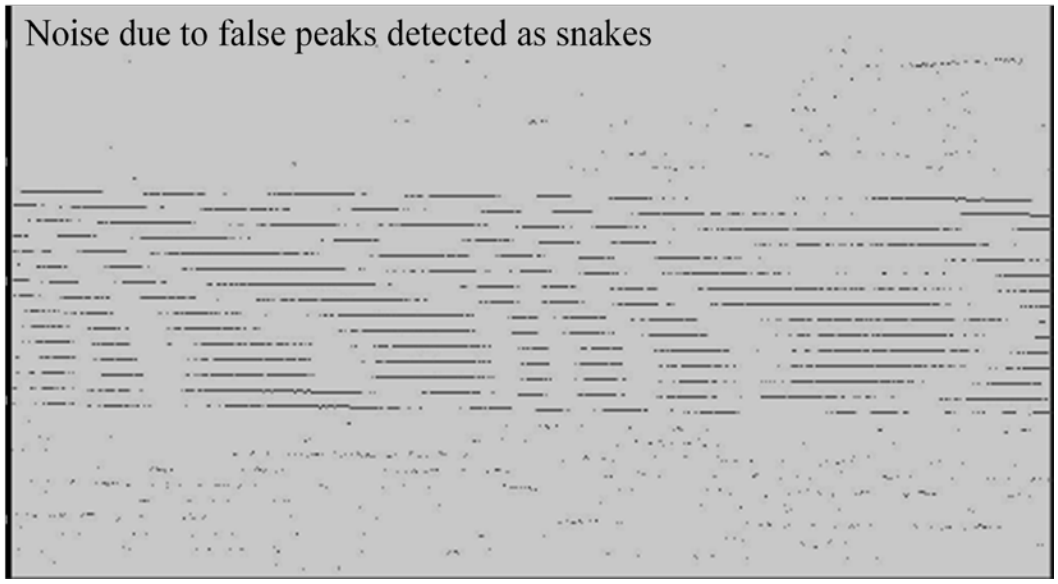

Figure 4. 12 Snakes with noise due to poor $Peak_{min}$ setting

Results from more reasonable settings of isolation parameters are indicated by the graphs in Fig's 4.13 and 4.14 illustrate positive and negative snakes detected by processing individual grayscale components of the image.

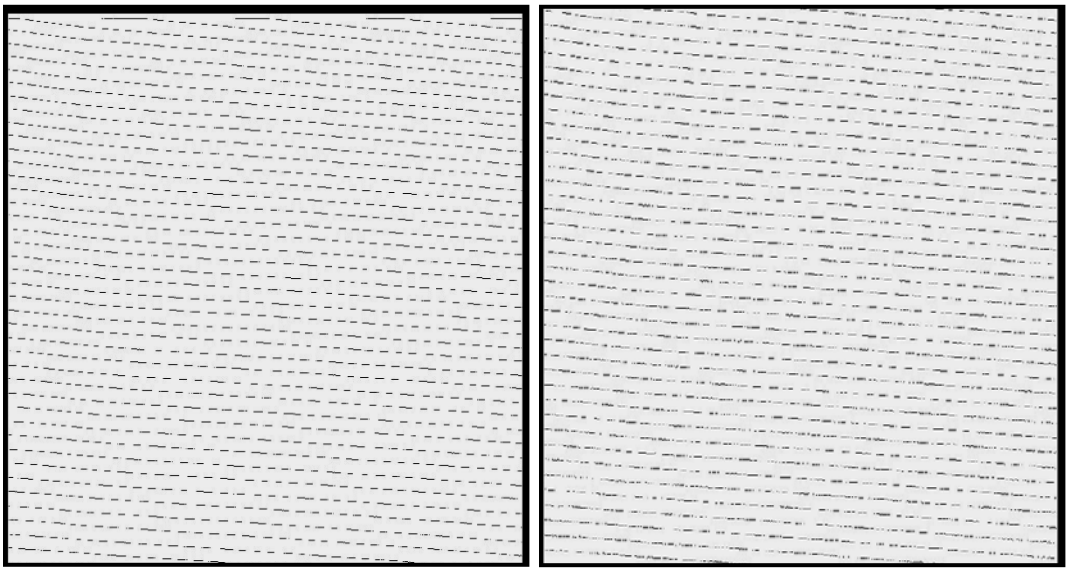

Figure 4. 13 Red channel Snake pattern – (a) Positive Peaks (b) Negative Peaks

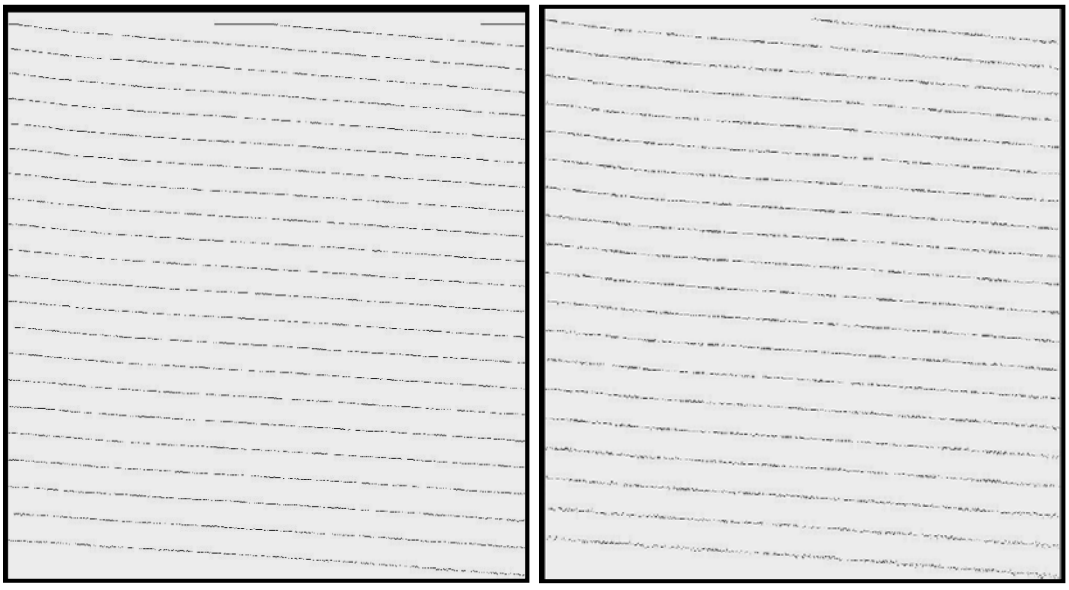

Figure 4. 14 Green channel Snake Pattern – (a) Positive Peaks (b) Negative Peaks

A cross sectional plot of the intensity of the middle column of the processed image is shown in Figure 4.15 and 4.16 for better visualization of the positive and negative peaks in the corresponding Red and Green channels snake images.

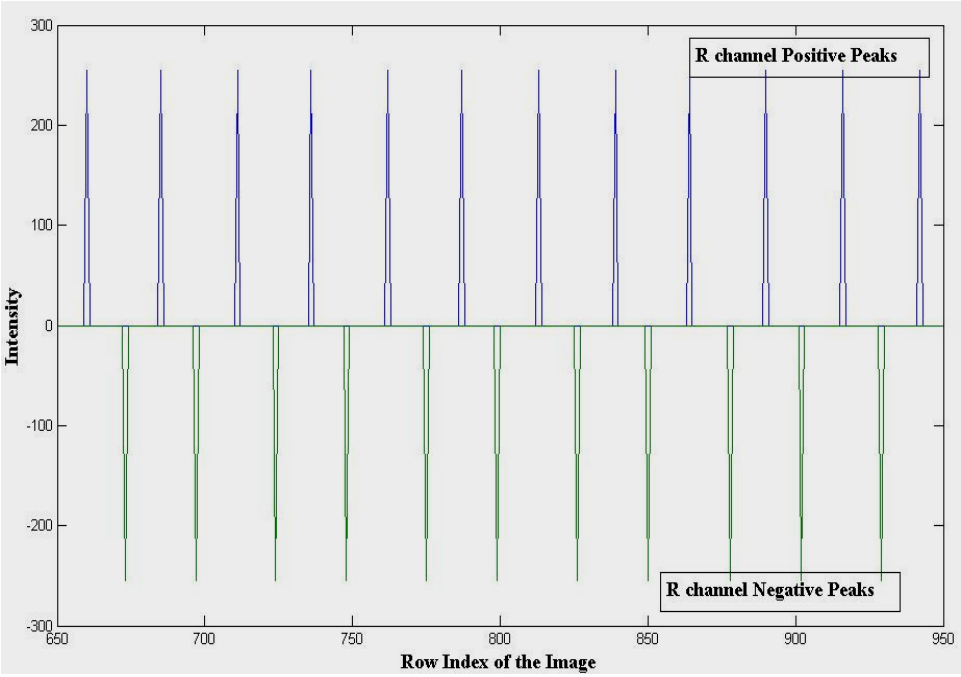

Figure 4. 15 Middle column Red channel positive and negative snakes

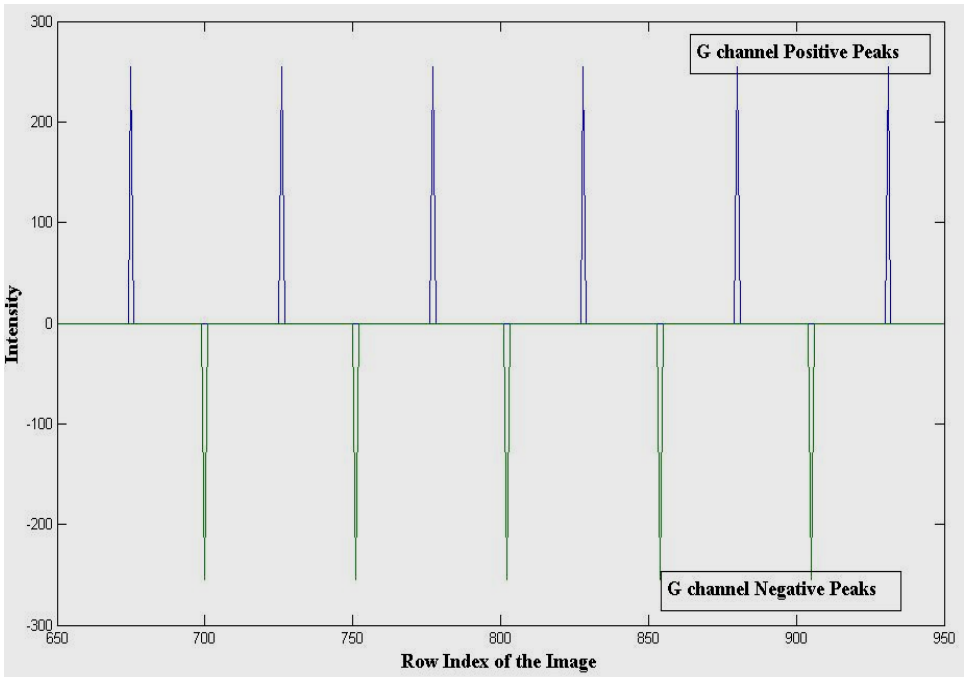

Figure 4. 16 Middle column Green channel positive and negative snakes

4.2.3 Post processing of wrapped phase

Fig 4.17 shows cropped image of phase extracted by processing snake images of individual grayscale components of the captured target image. It is observed that the phase map has non linear variation of phase caused due to snakes misalignment in red and green channels which define the boundary condition in the sub region for appropriate phase calculation. Also the white striped areas caused errors in the phase value shown in the cross-section across a column of phase map in Fig 4.18.

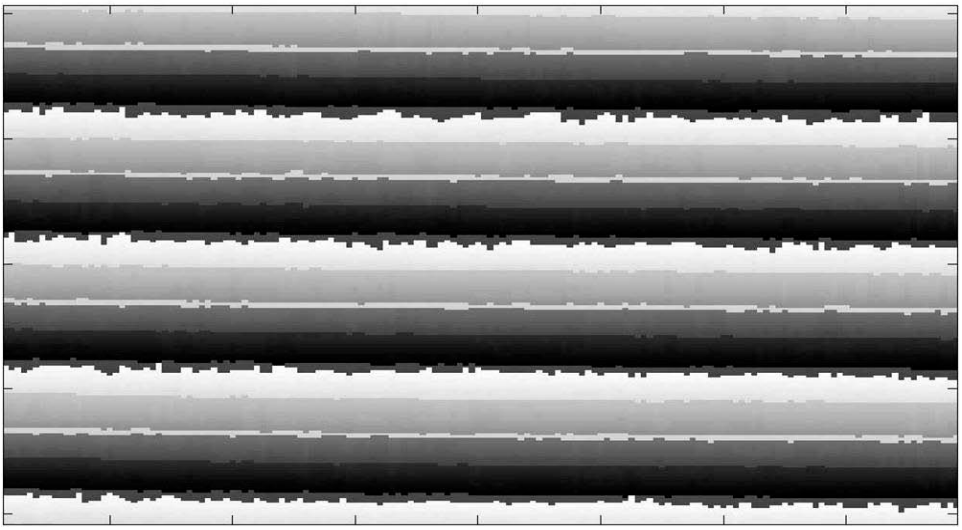

Figure 4. 17 Phase image of captured flat surface before snake misalignment in R and G channels

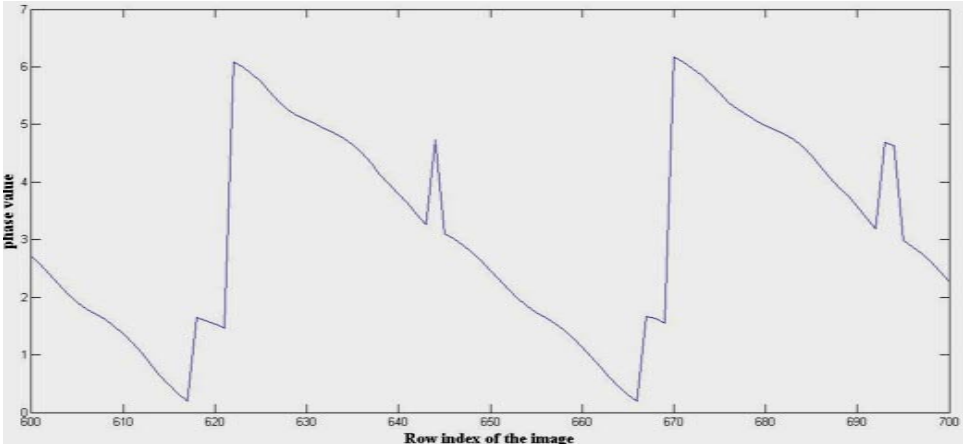

Figure 4. 18 Cross-section plot indicating error in phase value

Fig 4.19 is plotted with red and green channel snakes overlapped on the phase cross-section plot. It can be clearly seen the error in phase occurring with the misaligning peaks.

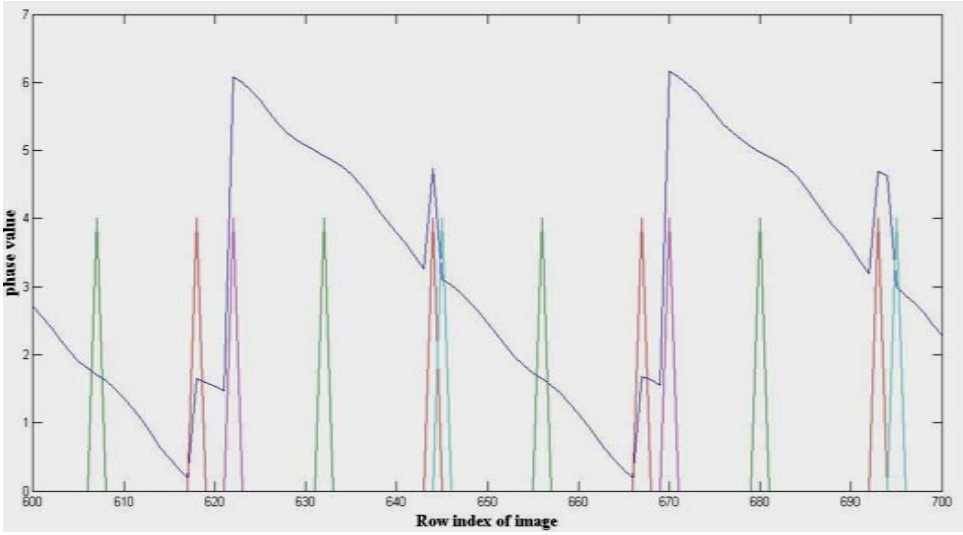

Figure 4. 19 Misalignment of snakes on the phase plot before correction

To align snakes a temporary image is created with red channel positive and negative snakes. Using imdilate function with prechosen structuring element, the green channel positive and negative snake images are dilated and combined with temporary image of red channel snakes to align their respective snakes position.

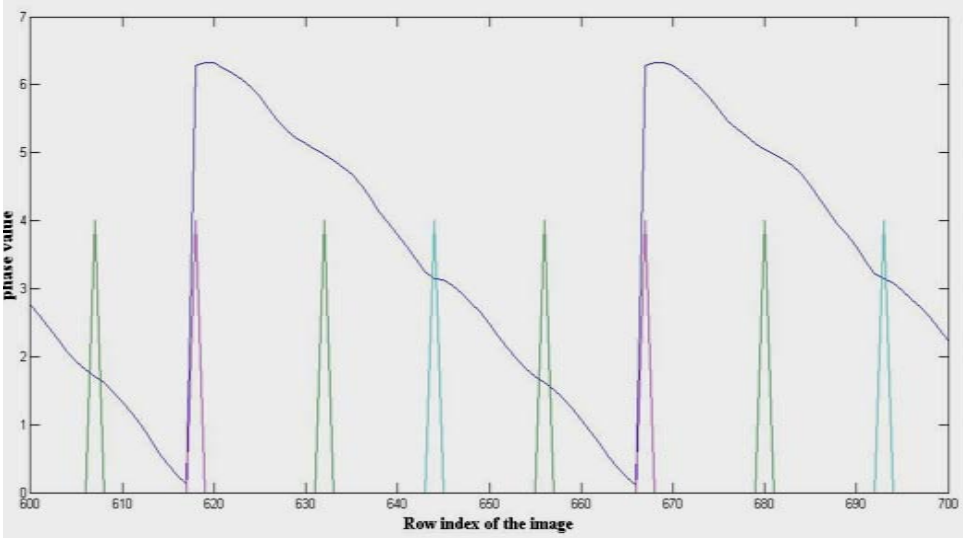

Figure 4. 20 Alignment of snakes on phase plot after correction

Fig 4.21 shows the error measured by taking the difference in the phase plots before and after snake alignment correction.

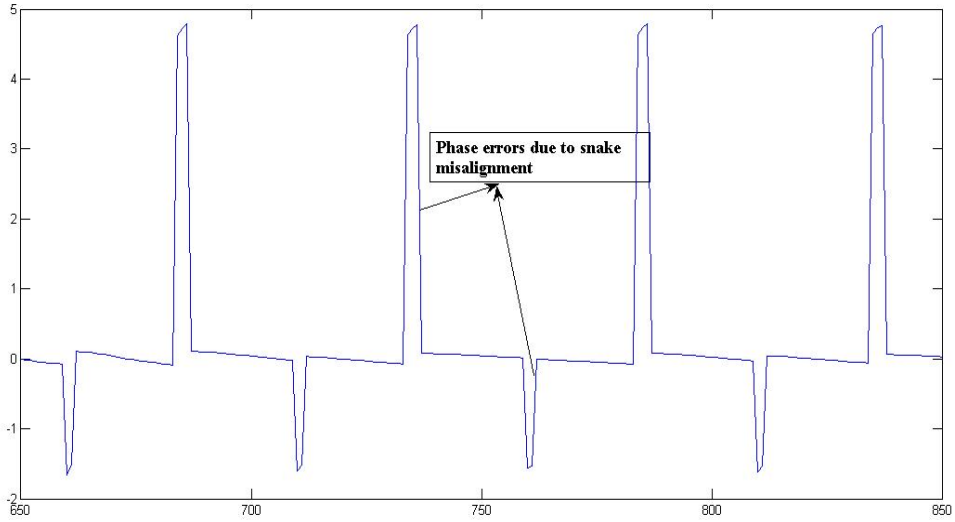

Figure 4. 21 Error measured before and after snake alignment correction

Fig 4.22 shows the cropped image of cleaned phase map of the image with proportionally varying phase wrapped around 0 to 2π according the ratio of intensities in red and green channel components of the input image with grayscale intensity vary between 0 to 255.

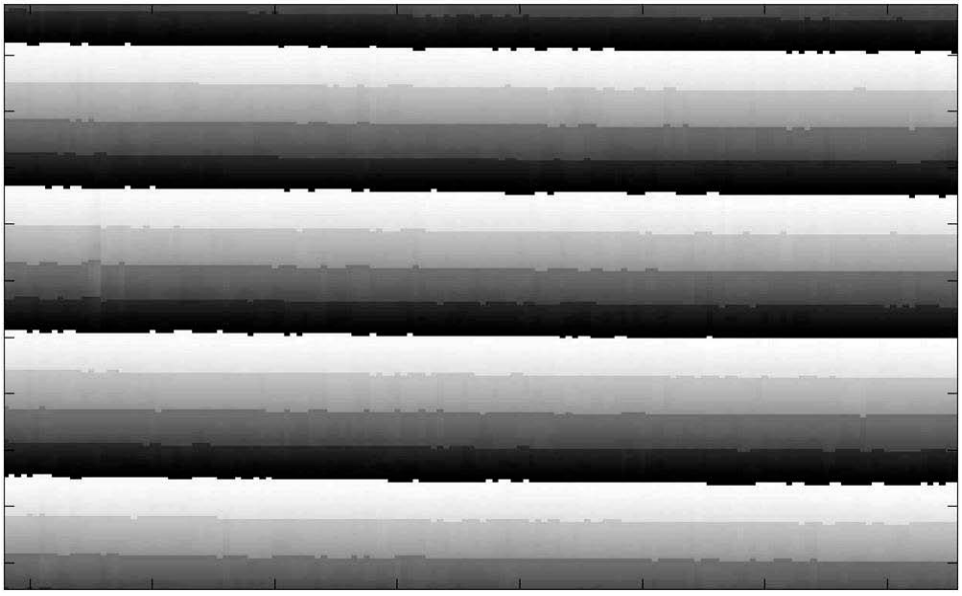

Figure 4. 22 Phase map after correction

4.2.4 Linear Interpolation

Fig 4.23 shows the unwrapped phase of the flat surface using the phase and and snake images. The vertical streaks spread across the unwrapped image are caused due to blank spots or holes in the snake image. In our algorithm, the snake count is used to unwrap the ambiguous phase on to a non-ambiguous scale. The error due to the holes is propagated through the entire column and corrupts the unwrapped phase.

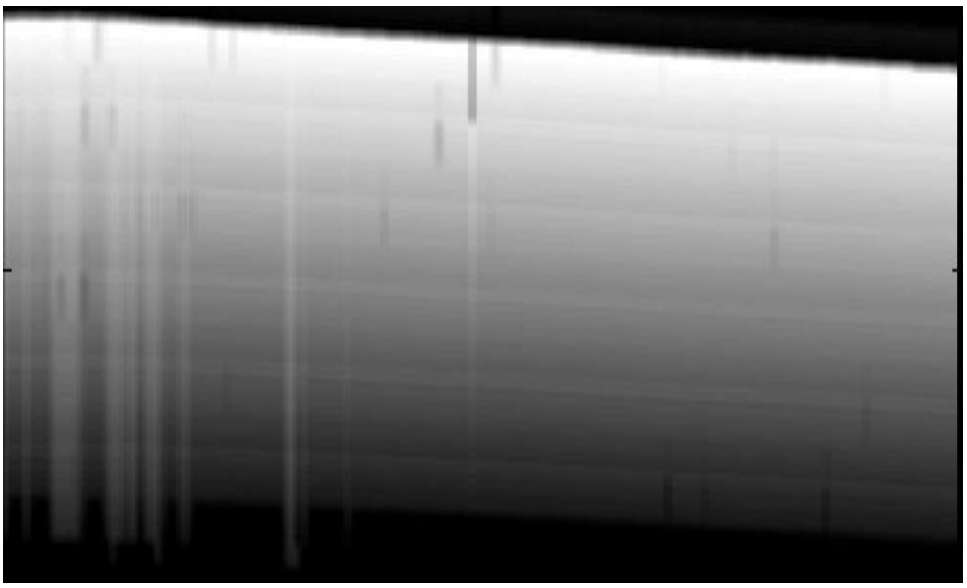

Figure 4. 23 Phase Unwrap plot of the captured image

In order to preserve accuracy, linear interpolation process is performed on the snake images. Using the snake identity matrix a pixel-based search is performed. For each nonzero snake pixel, a search within a user defined range attempts to identify the closest nearby snake. Using the two snake pixels as endpoints, a simple linear slope-intercept equation is used to sequentially assign appropriate values to each pixel between the two endpoints. This function fills the holes using a linear interpolation method.

$$m = (a * n) + b$$
$$m1 = (a * n1) + b$$
$$m2 = (a * n2) + b$$
$$a = (m1 - m2) \,/\, (n1 - n2)$$

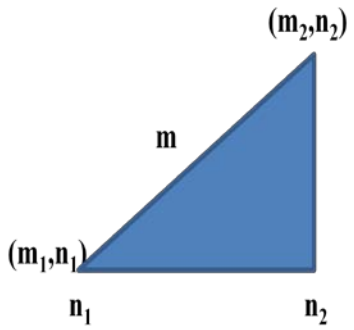

(4.3)

By substituting values of ‘a’ and ‘b’ we can find the slope m

Figure 4.24 and 4.25 illustrate the effect, with small cross-section of the snake across a single chosen column before and after linear interpolation respectively.

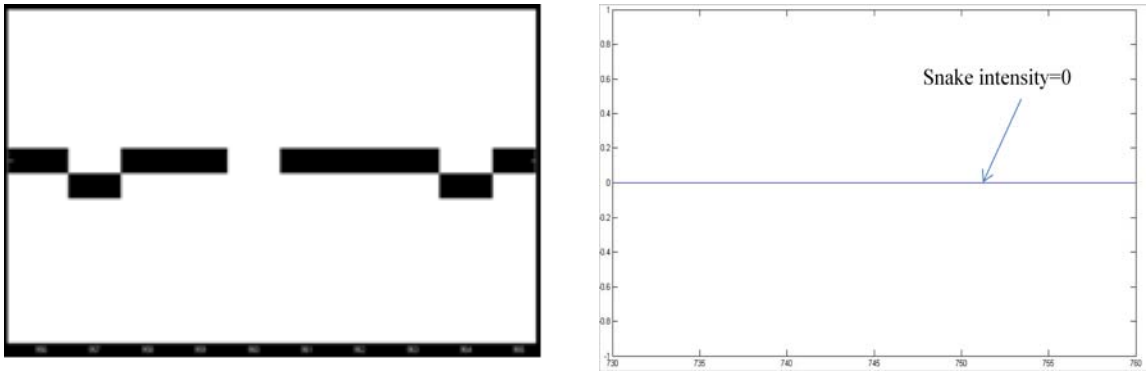

Figure 4. 24 Hole in the snake before Linear Interpolation – (a) 2D plot (b) Cross section showing absence of snake with intensity 0

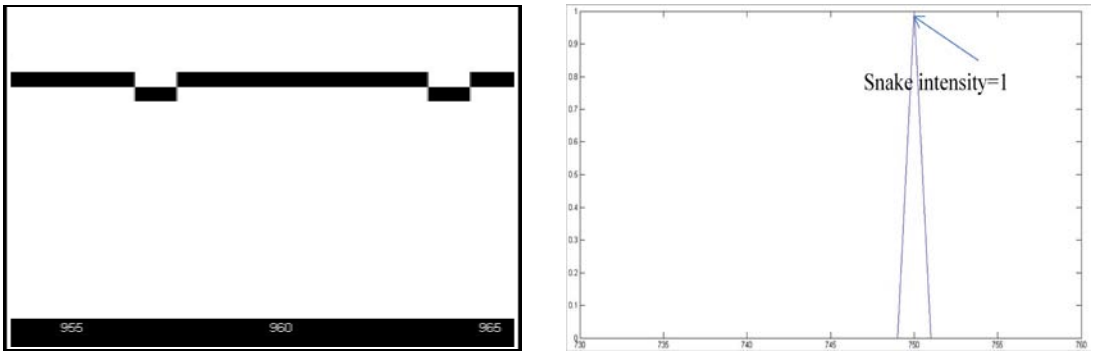

Figure 4. 25 Filled snake after Linear Interpolation – (a) 2D plot (b) Cross section showing snake with intensity 1

Figure 4.26 (a) indicates the cleaned out phase unwrapped image and Fig 4.27 shows the simultaneous plot of multiple column subsection is shown in this figure. The phase is ramping down from expected value of 2π.

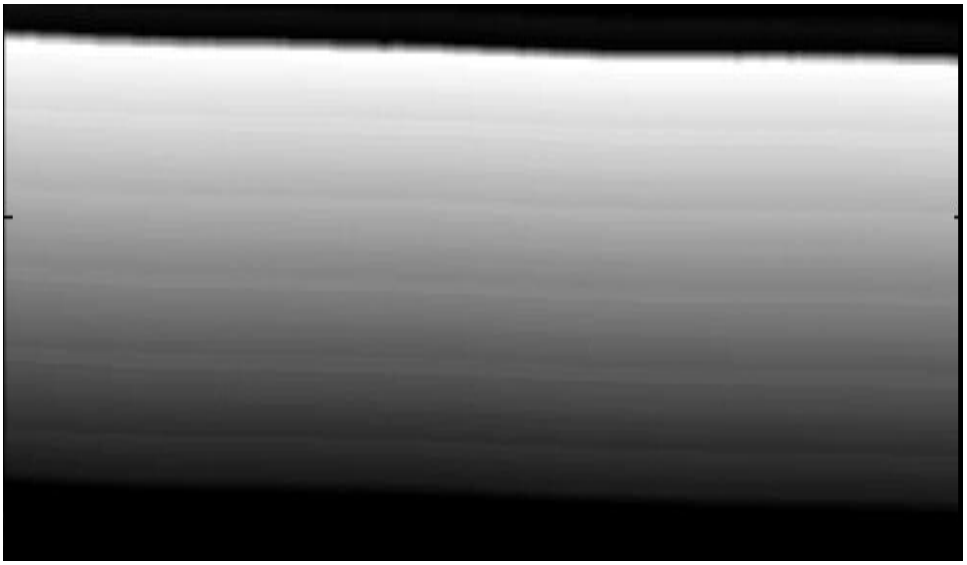

Figure 4. 26 Phase unwraped image after Linear interpolation

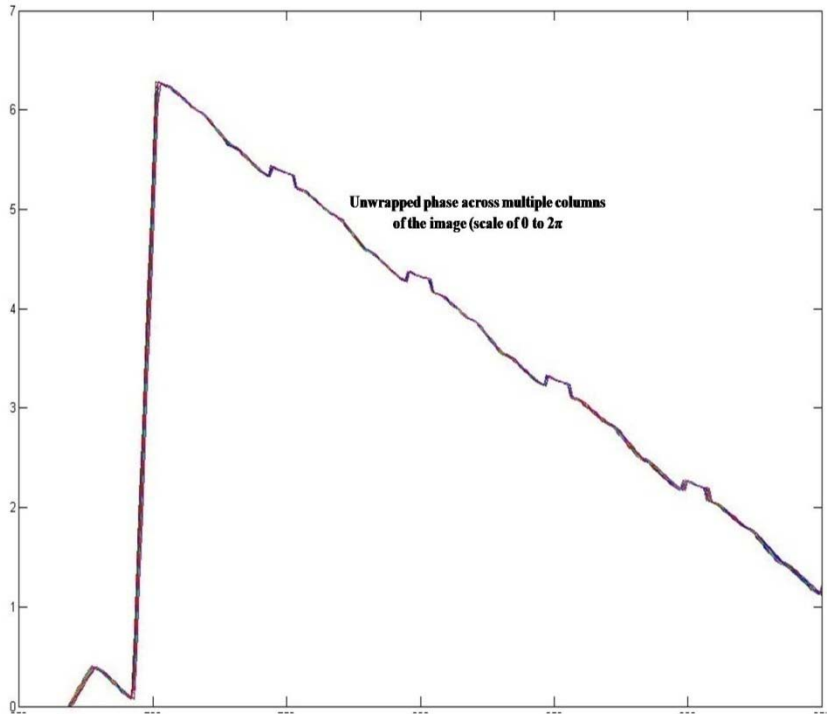

Figure 4. 27 Phase unwrapped section of multiple columns overlapped

4.3 3D Reconstruction

The main aim of this thesis is to use the color multiplexed single pattern to obtain 3D range information. After capturing the image and post processing, world coordinates are computed using calibration information for different target surfaces and the reconstruction results are presented in this chapter.

The 3D reconstruction can be summarized as follows.

- Project and capture the generated color pattern on a target object.
- Decode the image into three individual grayscale color channels.
- Isolate peaks and valleys to generate snake images.
- Calculate the phase using the snake positions and color channel ratios.
- Unwrap the phase to a non-ambiguous scale of 0 to 2π.
- Use the calibration equations 3.19 - 3.22 to obtain the 3D world coordinates.

4.3.1 Phase to world coordinates calibration

This section gives the details of equipment, the manual measurement of the pre-requisite parameters using flat surface and cosine manifold models as target subjects necessary for calibration. Calibration of a structured light system consists of a pin-hole camera (Canon 5.0 Mega Pixel, 1944x2592 pixel resolution) and a slide projector (Kodak Ektagraphic IIIA) with 1200x1800 pixel resolution) connected to a Polywell Windows XP computer. Based on the orientation of the structured light stripes, the projector is displaced vertically relative to the camera in space.

The Geometric parameters L, d and Δh should be manually chosen for calibration as explained in calibration experimental procedure of section 3.3. The focal length of the slide projector is 150mm. Based on the focal length/projector distance provided by the manufacturer [31]; we have chosen maximum distance L between the projector and the reference plane. Table 4.1 gives the details of experimental parameters.

Table 4. 1 Calibration setup parameters

Distance between projector and reference plane (L)	26.25 inches
Distance between camera and projector optical lens	8.0 inches
Distance between reference and moved plane	3 inches
Height of the cosine manifold(manual measurement)	2.25 inches

The subjects used in the calibration process are flat surface for reference plane and cosine manifold model as target object whose depth measurement is to be measured.

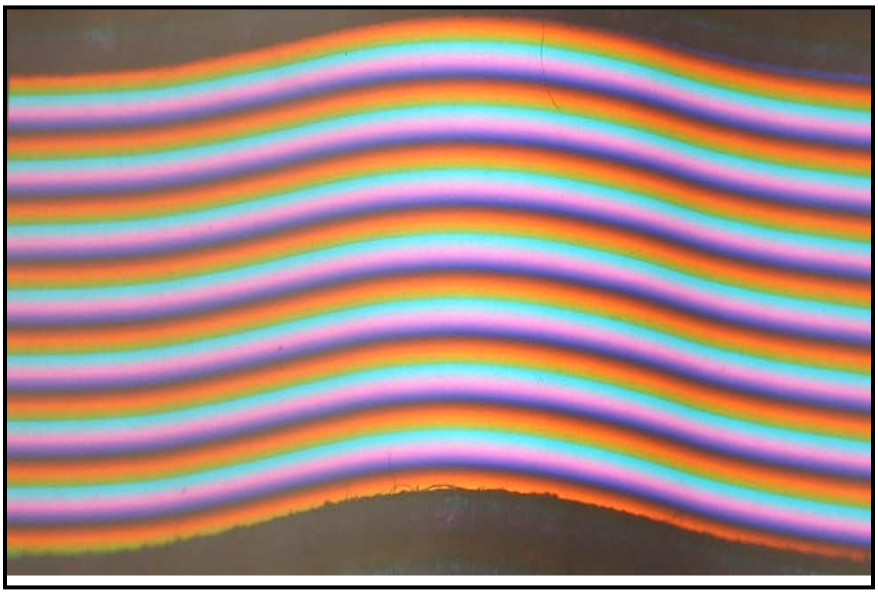

Figure 4. 28 Image of captured object (Cosine manifold) by projecting test pattern

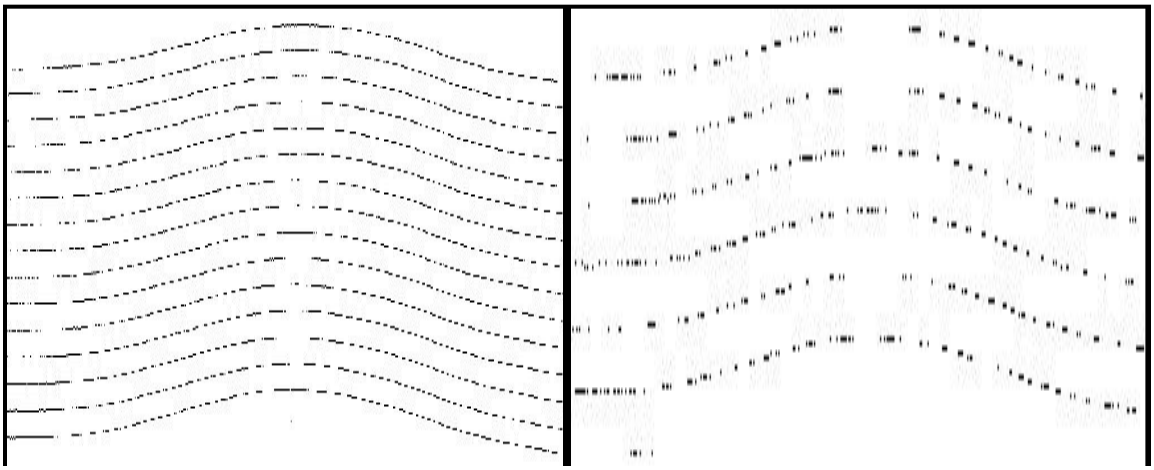

Figure 4. 29 Isolated Snake pattern in Red and Green channel respectively.

4.3.2 Reconstruction of flat surface and Cosine manifold

The world co-ordinate system is represented by $P^w = (X^w, Y^w, Z^w)$. In our system the target model is assumed to be defined as mm/pixel. But the captured image may not correspond to actual pixel difference as per the original object height. So the corresponding measurement is taken physically and updated in the 3D reconstruction process as given by Eq (4.3)

$$scale\_Factor = \frac{object\ \ height\ in\ mm}{pixel\ \ difference} \tag{4.3}$$

Thus X^w and Y^w are updated with the scale factor, while Z^w corresponds to the depth information of the target model.

The calibration experiments are performed on flat surface initially. The errors occurred are analyzed and corrected. The reference plane and move plane corresponds to the position of flat surface at a distance Δh. Fig 4.30 shows the reconstructed flat surface. But the surface is ramping instead of smooth due to scaling problem between phase to world coordinates.

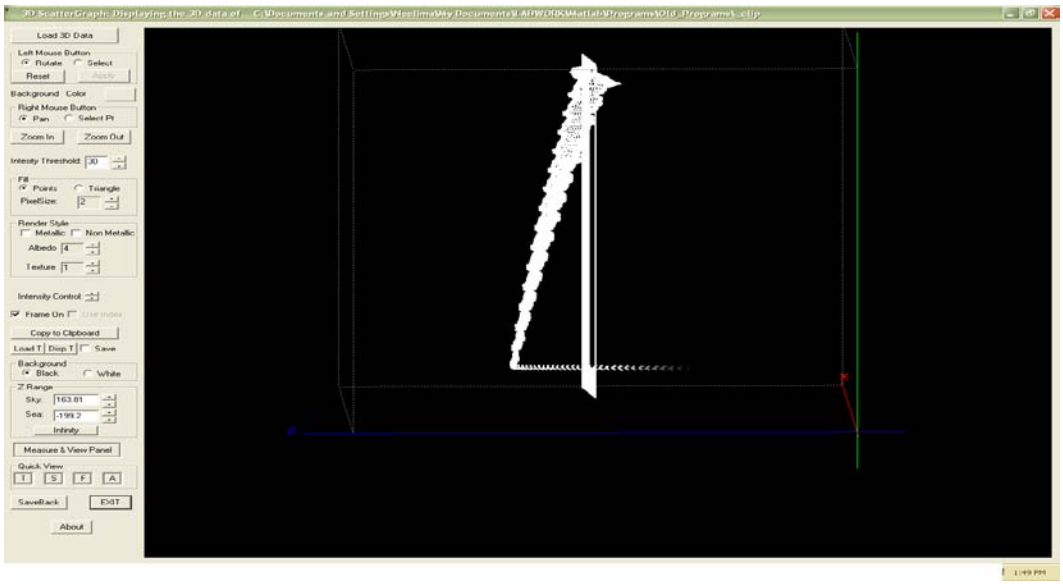

Figure 4. 30 3D plot of flat surface depicting the uneven scaling effect

As explained in section 3.4 the phase difference between the initial reference plane w.r.t to moved reference plane and object being measured are calculated to obtain geometric parameters β and *BC'*. The unwrapped phase is supposed to be varying with constant phase shift between the position of reference plane (initial and moved) to accurately calculate height of the surface using phase difference *BC'* as per equation 3.21. As illustrated figure 4.31 the error in scale while calculating height of the object.

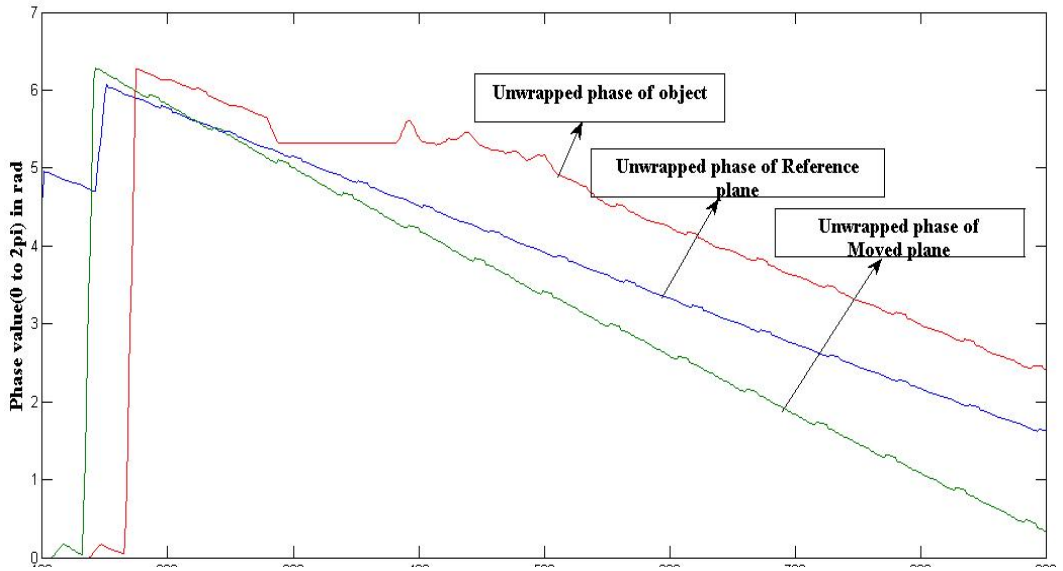

Figure 4. 31 Graph indicating the scaling problem

As explained in section 3.3.5 the offset matrix for phase unwrapping is obtaining by the counting the number of snakes across the captured image. If the snake count is different the error in scale occurs. So the calibration experiment is repeated by constraining the number of stripes in the projection pattern. This assures the snake count will be same for all the captured images irrespective of the subject position thus unwrapping on to same scale and hence corrected in Fig 4.32.

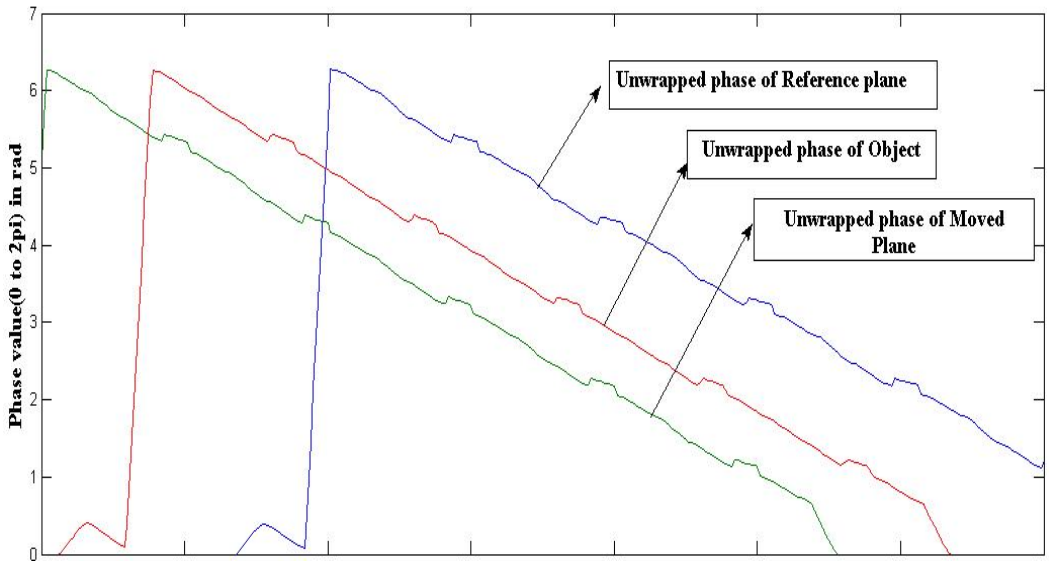

Figure 4. 32 Graph after removal of scaling problem

Fig 4.33 shows the reconstructed flat surface after correcting the scaling effect. It shows the ramping error is corrected.

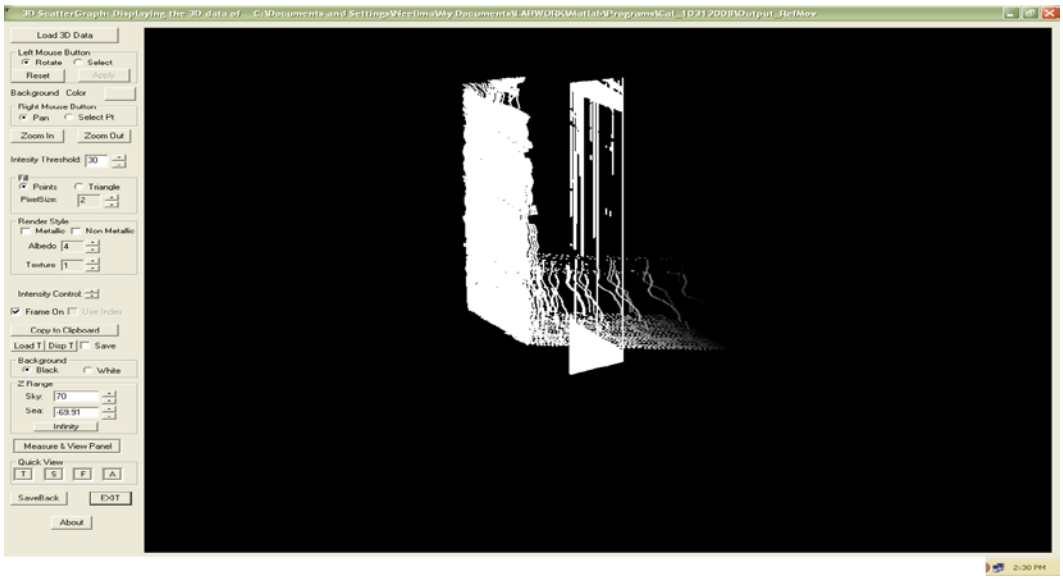

Figure 4. 33 3D plot of flat surface after removal of scaling effect

Fig 4.34 is the initial reconstructed image of flat surface. It clearly shows the error introduced due to holes in the snake detection process due to drop off in the unwrapped phase value as explained in section 4.2.3. The empty areas along the surface are due to unfilled snake stripes.

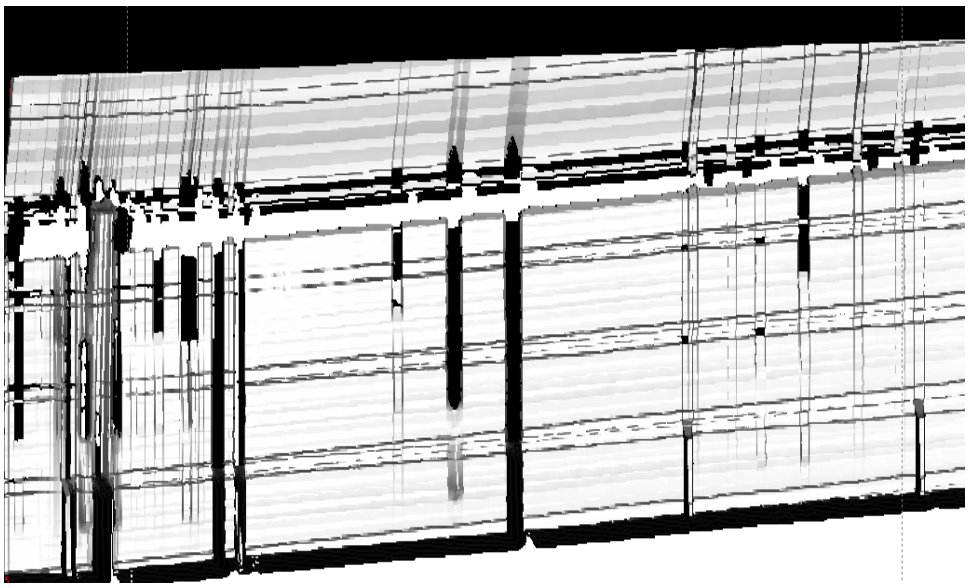

Figure 4. 34 3D plot of flat surface before linear interpolation

After filling the holes through linear interpolation the improvement in the 3D reconstructed image is illustrated in fig 4.35.

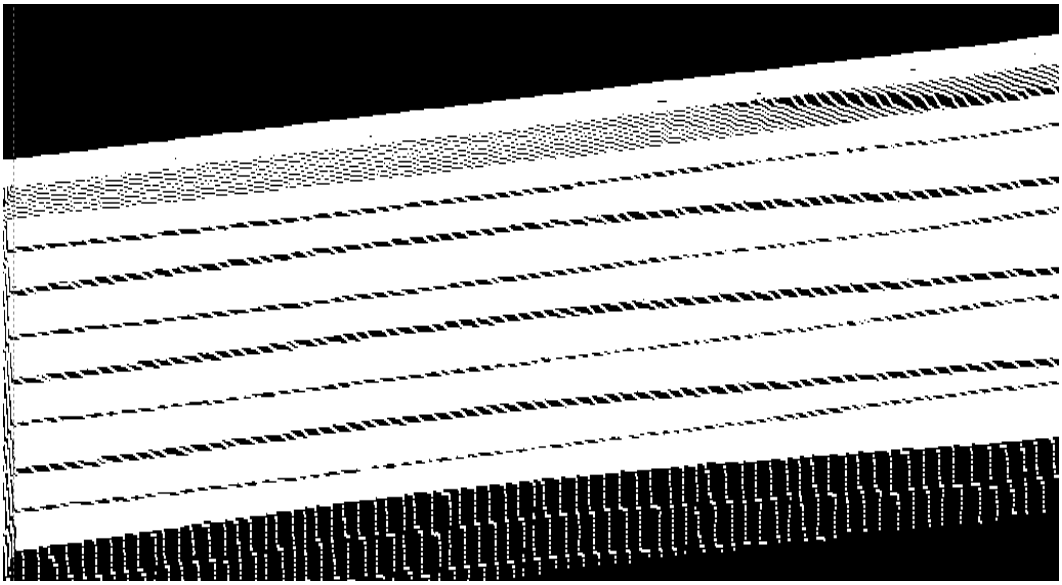

Figure 4. 35 3D plot of flat surface after linear interpolation

Due to calibration experimental anomalies the problem in the shape of 3D reconstructed image occurred which is seen as angularity in the reconstruction of flat surface and drop off in height towards the left edge in the surface reconstruction of cosine manifold shown in Fig's 4.36 and 4.37.

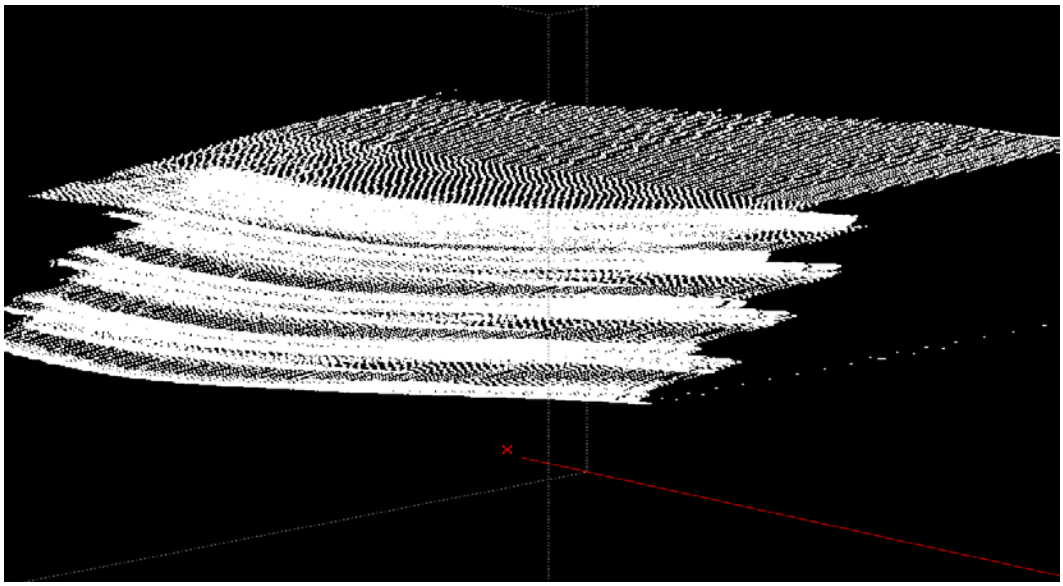

Figure 4. 36 3D plot of flat surface with angularity in reconstruction

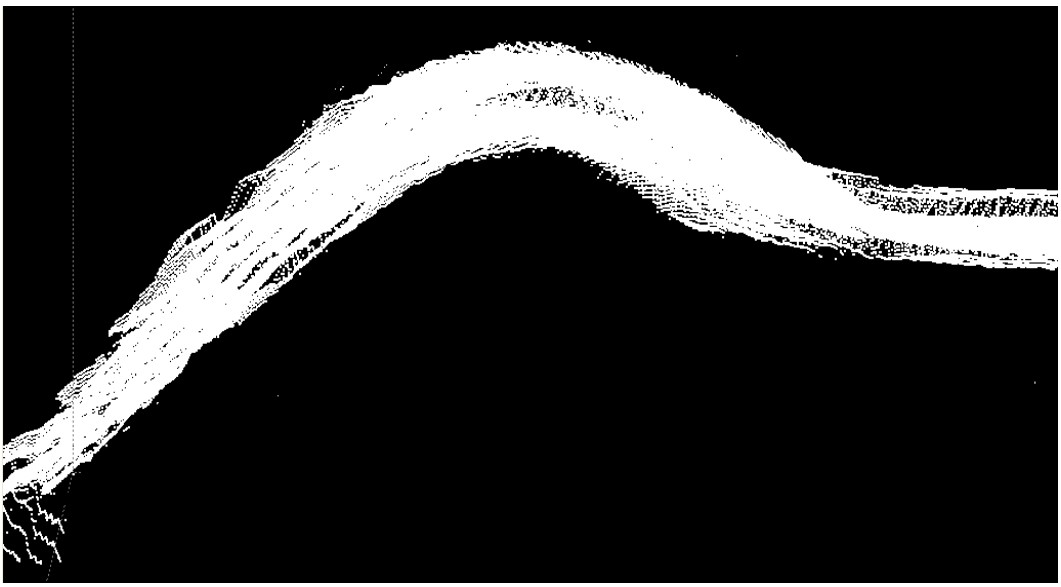

Figure 4. 37 3D plot showing drop off in object height towards left edge of cosine manifold surface in reconstruction

Fig's 4.38 and 4.39 shows the reconstructed image surface after recalibration and correction of angularity and drop off errors.

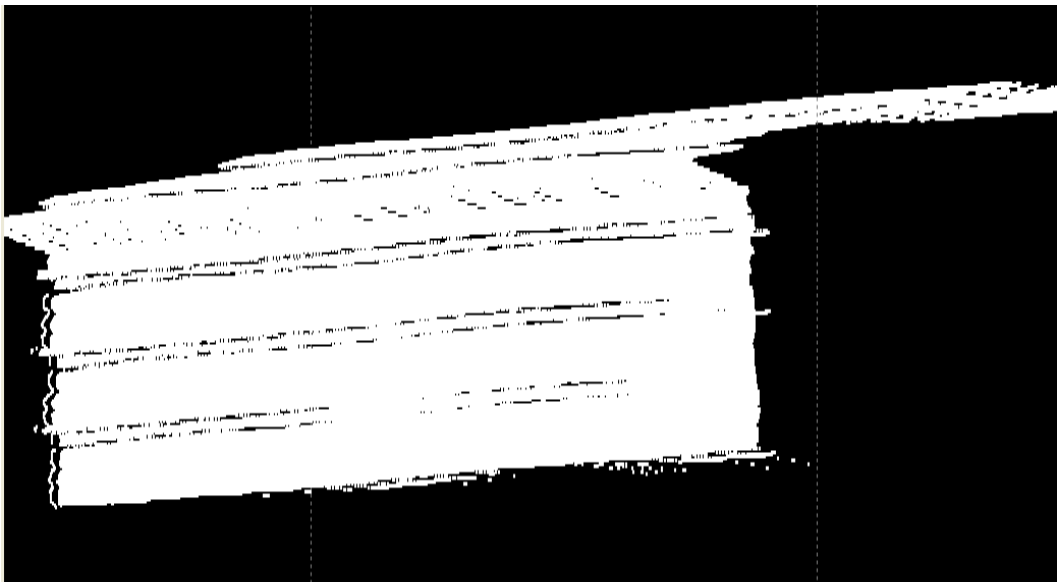

Figure 4. 38 3D plot showing correction in angularity of flat surface

Figure 4. 39 3D plot showing correction in object depth (left side)

Fig's 4.40 and 4.41 shows the reconstructed front view graphs of flat surface and the cosine manifold.

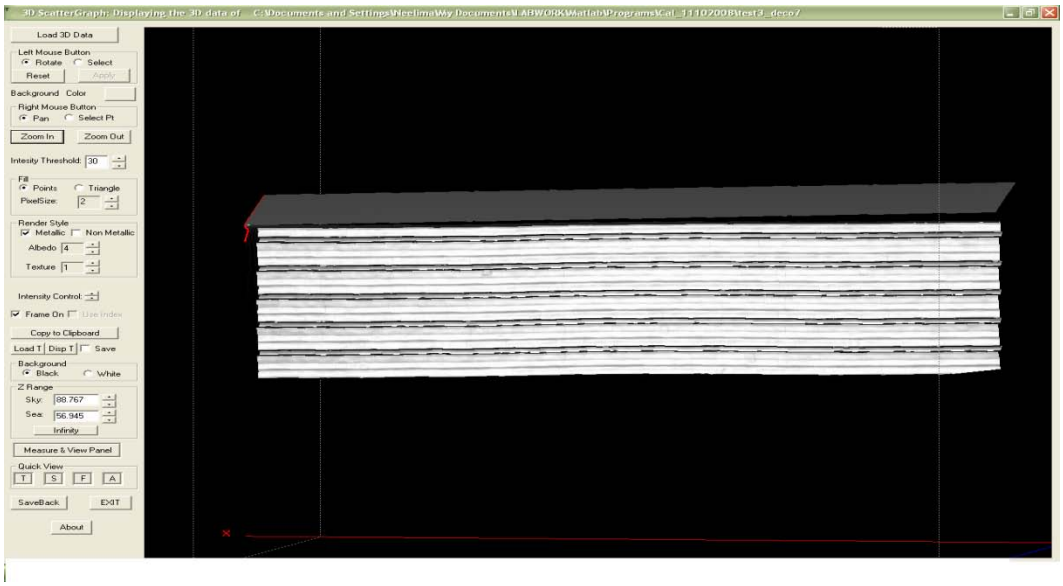

Figure 4. 40 3D plot showing front view of flat surface

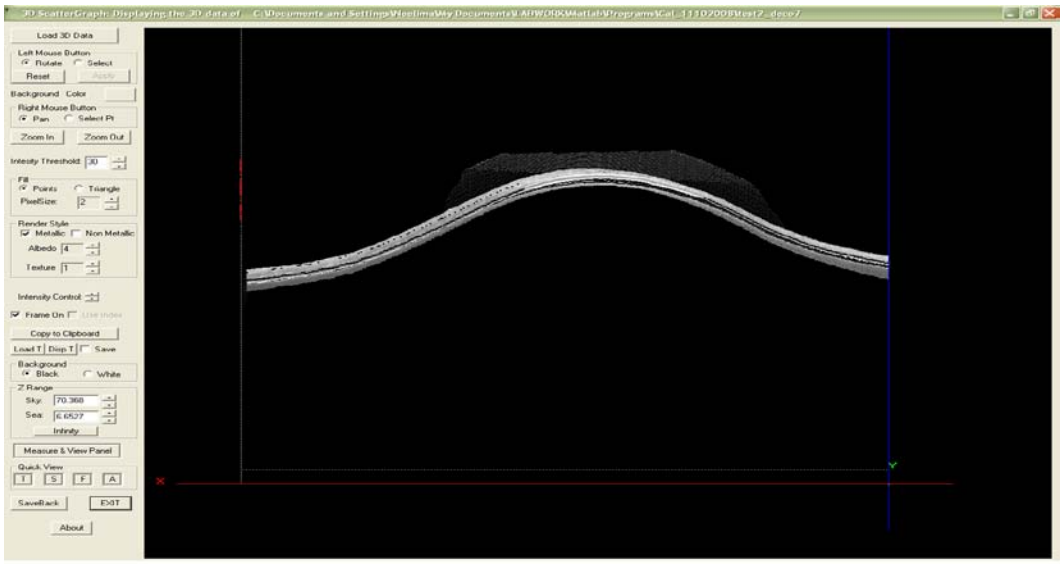

Figure 4. 41 3D plot showing front view of cosine manifold

Fig's 4.42 and 4.43 shows the reconstructed front and side view graphs of cosine manifold

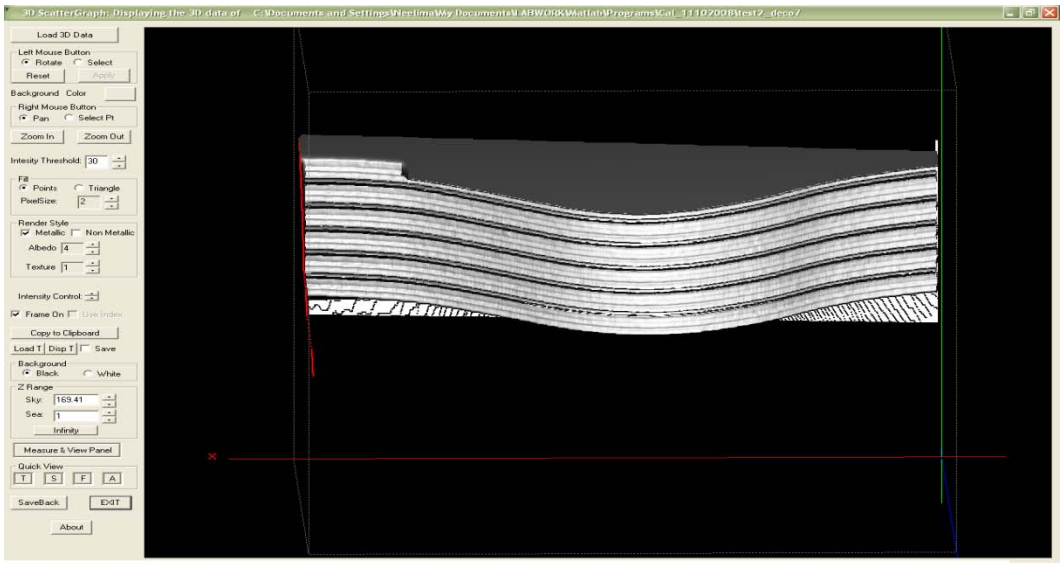

Figure 4. 42 3D plot showing 3D reconstructed cosine manifold

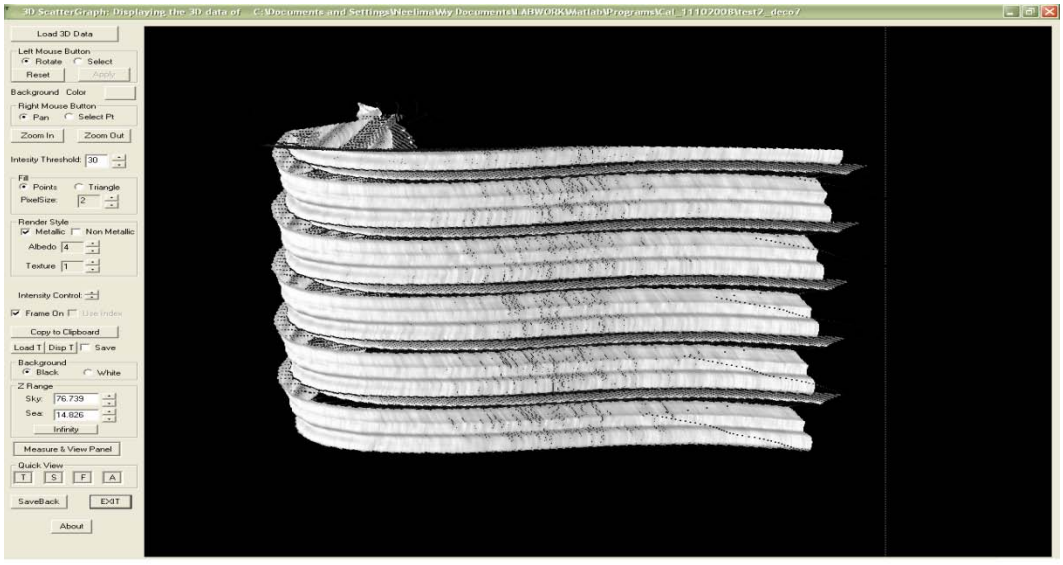

Figure 4. 43 Cropped side view of the 3D reconstructed cosine manifold model

Finally the comparison of expected height manually towards experimental observation of the target objects is given in table 4.2

Table 4. 2 Height map details of objects measured

Object	Height measurement in inches	
	Manual	Experimental
Flat Surface	3inches	3.227inches
Cosine manifold	2.25inches	2.48inches

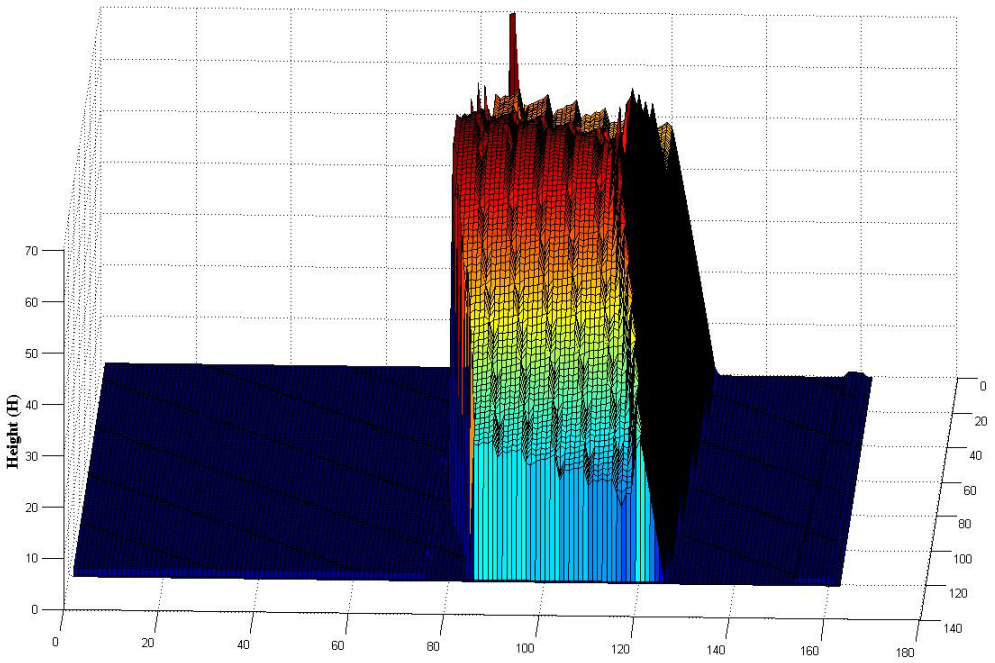

Figure 4. 44 3D height reconstruction profile of the object

Chapter 5 Conclusion and Future work

We introduced and explained a new “color multiplexing” technique which allows single-image SLI 3D reconstruction. The main goal of the research work, establishing viability of designed color pattern was achieved by successful depth extraction of the object under measurement. The optical triangulation method was developed using a simple slide projector and digital camera, thus reducing hardware costs. Theory and analysis of various processing algorithms are detailed, and results are presented. Additionally, experimental error measurements were performed in order to estimate errors introduced by key pattern features and improvements were made.

5.1 Conclusion

Use of SLI is a practical and simple solution to non-contact measurement. It avoids the correspondence problem of stereo vision and cost of time of flight techniques, which lack close range accuracy. The single pattern method described in this research allows use of high resolution digital cameras for one-shot image capture and in principle is capable of a 3D frame rate equal to that of the camera used. We have overcome the limitation of digital projector color filters that introduced inter-color interference by using a slide based projection. Use of triangular snake stripes in the projection pattern helped to enhance results with their higher peak-to-side-lobe ratio. The positive snake peaks with higher signal-to-noise ratio and linear interpolation between successive snake peak locations improves the accuracy in calculating phase information. Also by being able to encode more information effectively using multiple color channels with unique subpatterns for each we were able to get uninterrupted phase information, thus increasing the depth accuracy and overcoming some of the drawbacks of other spatial encoding techniques. The proposed color pattern method utilizes the ratio of Red and Green channel intensities between successive peaks for phase extraction to overcome albedo sensitivity and object surface reflectance to some degree. It computes a non-ambiguous depth map from a single snapshot of the scene illuminated by the pattern. The method adopted provides improvement over existing implementations which require significant processing time. The simple geometric calibration technique which was newly integrated

into this research work obtained good results with sufficient accuracy in depth information of the object.

5.2 Future Work

This thesis work is mainly confined to implementation and testing for the viability of this color multiplexed single pattern technique. Being proven as a promising candidate for 3D data acquisition, this method has potential for future research particularly in biometrics. Although the current snake peak detection strategy works with good accuracy, future developments are likely to include improvement in snake identity by use of sub-pixel snake peak position measurements. Design of more robust algorithms may be necessary to mitigate the effect of banding artifacts introduced due to non-linearity or rounding around the peaks of the triangular subpattern of the captured image of each channel due to hardware limitations. As the main application beyond design of this technique is biometric measurement of the human hand, for measuring friction ridge variation. Being that the surface nature of human skin contains less blue reflectance more emphasis is given to red and green channel components in extracting the required phase information. The blue channel is not used, but we left for future exploration of its potential to double the non-ambiguous range.

Appendix: Matlab Code

```
// Common Input Parameters for all the functions:
// M - Row index of the image
// N - Column index of the image
// A –  Pixel intensity values of Captured image
// Ar,Ag,Ab – Grayscale components of the R,G and B channels of the captured image.
//-----------------------------------------------------------------------------------------------------
```

Design of projection Pattern

```
%{ Function to  create unique subpatterns for each color channel
Input parameters : M, N , Kp- No of cycles per field of view in projection pattern
function  f1=CreatePattern(columns, rows, cycles)
%Rows and Columns in the bitmap image.
 M=rows;
 N=columns;
%period Tc = M/kp where kp=no of cycles per field of view value
kp=cycles;
Tc=floor(M/kp);   %No of pixels per stripe

% Matrix used to fill cycles for three color channels RGB
cycle1=zeros(Tc,N);
cycle2=zeros(Tc,N);
cycle3=zeros(Tc,N);
nd=4*(floor(Tc/4)); %Number of pixels in the image

%constructing the triangular stripe subpattern for Red channel
x1=1:Tc/4;
for n=1:N
        cycle1(1:nd/4,n)=x1;
        cycle1(nd/4+1:nd/2,n)=Tc/4-x1;
        cycle1(nd/2+1:0.75*nd,n)=x1;
        cycle1(0.75*nd+1:nd,n)=Tc/4-x1;
end
%Normalize the wave
cycle1=cycle1./(max(max(cycle1)));
%To convert into a bitmap all values are scaled to between 0 and 255
cycle1=cycle1.*255;

 %constructing the triangular stripe subpattern for Green channel
x2=1:Tc/2;
for n=1:N
        cycle2(1:nd/2,n)=x2;
        cycle2(nd/2+1:nd,n)=Tc/2-x2;
end
cycle2=cycle2./(max(max(cycle2)));
```

```
cycle2=cycle2.*255;
 %consturcting the subpattern for Blue channel
for n=1:N
cycle3(1:nd/2,n)=1;
cycle3(nd/2+1:nd,n)=0;
end
cycle3=cycle3./(max(max(cycle3)));
cycle3=cycle3.*255;
%Matrix to store final bitmap image
out=zeros(M,N,3);

%Repeating the function across the image
size(cycle1)
for n=1:kp
   out((n-1)*Tc+1:n*Tc,:,1)=cycle1;
   out((n-1)*Tc+1:n*Tc,:,2)=cycle2;
   out((n-1)*Tc+1:n*Tc,:,3)=cycle3;
end;
f1=uint8(out);
figure(1),imshow(f1);colormap;
%}

A=double(imread('c:\DocumentsandSettings\Neelima\MyDocuments\LABWORK\Matla
b\Results\Capture_Image.JPG'));
[M,N,P]=size(A);
A=imresize(A,[floor(M/2),floor(N/2)]);
Ar=A(:,:,1);
Ag=A(:,:,2);
Ab=A(:,:,3);
clear A;
```

Positive Snake Detection

```
%{ This function attempts to find maximum intensity value of the subpattern in each
channel and isolate positive snakes by using Peak to side lobe ratio matrix calculated
using sidelobe intensities defined within search range and thresholded using PSRmin and
Peakmin
function X=PositivePeaks(B, Pd, PSRmin,Peakmin)
%B is grayscale image, Pd indicates sidelobe distance, Pd, Peakmin depends on the
image and PSRmin=1.02 -> 1.30
Bx=double(B);
Bx=Bx./max(max(Bx));   % Normalizing the matrix.

%Calculating the PSR using sidelobe ratio
Pd=abs(Pd);
[M N]=size(B);
```

```
C=zeros(size(B));      %Initialising matrix to hold PSR values .
A=C;
for m=1:M                % m=vertical row number.
   for n=1:N             %n=space along columns ie. horizontal space.
      flag=0;
      y1=m-Pd;
       y2=m+Pd;
       if y1<1
         flag=1;
      end
      if y2>M
         flag=1;
      end
      if flag==0
         sidelobe=Bx(y1,n);
         if Bx(y2,n)>sidelobe
            sidelobe=Bx(y2,n);      % PSR takes the intensity ratio of value with the
                                       pixel    under consideration
          end
          if sidelobe>0
                  PSR=Bx(m,n)/sidelobe;
         else if B(m,n)==0
                  PSR=0;          %It evaluates any minimum pixel points
          else
                 PSR=0;
          end
        end
         C(m,n)=PSR;             %Matrix to store all PSR ratios
      end
   end
end

% Generating  a binary mask by using threshold values of PSRmin and Peakmin
%to filter out low intensity and false peaks.
A(find((C>=PSRmin)&(B>=PeakMin)))=1;
 E=C;
C=C.*A;
D=zeros(size(B));

% Routine to assign 1's to potential positive peaks using PSR ratio matrix after
thresholding i.e C and binary mask A
for n=1:N
   start=0;
   fmax=0;
   for m=1:M
      if (A(m,n)==1)&(start==0)
```

```
        start=1;
        fmax=C(m,n);      %Find max PSR values from C matrix and assigns it to
                             fmax
        posmax=m;         % Positive peak is stored in Posmax
      end
      if (start==1)&(A(m,n)==0)
        start=0;
        D(posmax,n)=1;   %At posmax location set the intensity value to 1.
        fmax=0;
      end
      if (start==1)&(A(m,n)==1)
           if C(m,n)>fmax         %check if the PSR is the maximum encountered in
                                    the section
             fmax=C(m,n);
            posmax=m;
          end
      end
   end
end
X=D;
Ar_temp=B/(max(max(B)));
E(find(E<PSRmin))=0;
figure(1)
 plot(650:900, E(650:900,700),650:900,1.2*X(650:900,700)); %}
```

Negative Snake Detection

```
%{ This function attempts to find minimum intensity value of subpattern by using a pixel
based search between two positive peaks of a snake with prechosen search range.
function X=NegativePeaks( B,positivepeaks, Pd)

Bx=double(B);
Bx=Bx./max(max(Bx));
 Pd=abs(Pd);
[M N]=size(B);
grown1=positivepeaks;

%This routine basically searches for a negative pixel(minimum value) between two
consecutive positive pixels with in the search range indicated by the variable "range".
range = Pd;
out =zeros(M,N);
for n=1:N-1
   for m=range+1:M-range
      if grown1(m,n)>0
        found=0;
        temp=0;
```

```
            minval =256;
            negpeakloc=m;
            for j=floor(range/5):range
                if grown1(m+j,n)>0 && found==0
                  found = 1;
                  temp=j;
                end
            end
            if found == 1
              for j=1:temp-1
                 if Bx(m+j,n)< minval
                   minval=Bx(m+j,n);
                   negpeakloc=m+j;
                 end
              end
              if negpeakloc ~= m
                 out(negpeakloc ,n)=1;      %Finally setting value 1 to all negative pixel
locations forming negative snakes matrix
              end
            end
         end
    end
end
X=out;
%}
```

Phase_Extraction

```
%{ Creates a phase matrix from the gray scale components of R & G channels using their
respective snake images. The output of the function is a completed Color Pattern phase
image of the captured object.
function P=PhaseRGB(Rp,Rn,Gp,Gn,Bp,Bn,range,Ar,Ag)
[M,N]= size(Rp);

%Aligning Green and Red channel snakes (both positive and negative)
 T1=Rp|Rn;
 n=10;
 Gx=imdilate(Gp,ones(n,n));
 Gp=Gx&T1;
 Gx=imdilate(Gn,ones(n,n));
 Gn=Gx&T1;

%Routine to fill matrix X with slope values for RED channel between successive positive
and negative peak%
Yp=0;Yn=0; a=0; b=0;d=0;
X=zeros(M,N,3);
for n=1:N
```

```
for m=range+1:M-range
   foundnegpeak=0;
   if Rp(m,n)>0
      Yp=m;
     for i=1:range
        if Rn(m+i,n)>0
            Yn=m+i;
            foundnegpeak=1;
        end
     end
     if (foundnegpeak==1)
         a=255/(Yn-Yp);
         b=Ar(Yn,n);
         d=Ar(Yp,n);
       for Y=Yp:Yn
          X(Y,n,1)=a;
          X(Y,n,2)=b;
          X(Y,n,3)=d;

       end
     end
   end
   foundpospeak=0;
   if Rn(m,n)>0
      Yn=m;
     for i=1:range
        if Rp(m+i,n)>0
            Yp=m+i;
            foundpospeak=1;
        end
     end
     if (foundpospeak==1)
         a=255/(Yn-Yp);
         b=Ar(Yn,n);
         d=Ar(Yp,n);
       for Y=Yn:Yp
          X(Y,n,1)=a;
          X(Y,n,2)=b;
          X(Y,n,3)=d;

       end
     end
   end

end
```

```
end

%Routine to fill matrix X with slope values for RED channel between successive positive
and negative peak%
 [M,N]= size(Gp);
range=2*range;
Yp=0;Yn=0; a=0; b=0; d=0;
Z=zeros(M,N,3);
for n=1:N
   for m=range+1:M-range
      foundnegpeak=0;
      if Gp(m,n)>0
         Yp=m;
        for i=1:range
           if Gn(m+i,n)>0
              Yn=m+i;
              foundnegpeak=1;
           end
        end
        if (foundnegpeak==1)
            a=255/(Yn-Yp);
            b=Ag(Yn,n);
            d=Ag(Yp,n);
          for Y=Yp:Yn
             Z(Y,n,1)=a;
             Z(Y,n,2)=b;
             Z(Y,n,3)=d;

          end
        end
      end
      foundpospeak=0;
      if Gn(m,n)>0
         Yn=m;
        for i=1:range
          if Gp(m+i,n)>0
              Yp=m+i;
              foundpospeak=1;
           end
        end
        if (foundpospeak==1)
            a=255/(Yn-Yp);
            b=Ag(Yn,n);
            d=Ag(Yp,n);
          for Y=Yn:Yp
             Z(Y,n,1)=a;
```

```
            Z(Y,n,2)=b;
            Z(Y,n,3)=d;

          end
        end
      end

  end

end

%Calculating Phase by using the slope orientation defined for R & G channels
ph=zeros(M,N);
Io=255;
% Normalizing Ar and Ag intensity values to be between 0 and 255.
Ar=255*(Ar./(X(:,:,3)))- (X(:,:,2));
Ag=255*(Ag./(Z(:,:,3)))- (Z(:,:,2));
x=0;
for n=1:N
  for m=1:M
      x=0;
      a=X(m,n,1);
      b1=X(m,n,2);
      b2=Z(m,n,2);
      c=Z(m,n,1);
      d1=X(m,n,3);
      d2=Z(m,n,3);
      r=Ar(m,n);
      g=Ag(m,n);

      if(a>0 && c>0)
         x=(r)+(2*g);
         ph(m,n)=((x/(d1+d2))* (pi/2)) ;
      end
      if(a<0 && c>0)
         x=(d1-r)+(2*(g-(d2/2)));
         ph(m,n)=(((x/(d1+d2))* (pi/2))) + pi/2  ;

       end
     if(a>0 && c<0)
         x=r+(2*(d2-g));
         ph(m,n)=(((x/(d1+d2))* (pi/2))) + pi;

      end
      if(a<0 && c<0)
         x=(d1-r)+(2*((d2/2)-g));
```

```
        ph(m,n)=(((x/(d1+d2))* (pi/2))) +((3*pi)/2);

      end
   end
end

 P=ph;
 figure(1), imagesc(P),colormap gray;
```

Phase_Unwrapping

```
%{ Creates a phase unwrapped matrix from the Phase matrix and R& G snake images
The output of the function is a completed Color Pattern phase unwrapped image of the
captured object for calculating phase to world coordinates. This program counts the
snakes to form an offset image and combine with phase image to obtain non-ambiguous
phase map between 0 and 2pi.
 function PU=Phase_Unwrap(Rp,Rn,Gp,Gn,Bp,Bn,range,Ar,Ag,P)
[M,N]= size(Rp);
 ph=P;
 peakfound1=0; peakfound2=0; peakfound3=0;
  X=zeros(M,N);
  for n=1:N
    offset=0;
   for m=M-range:-1:range
       if(Rn(m,n)>0 && peakfound1==0)
          for j=-range:range
             if(Gn(m+j,n)>0)
                peakfound1=1;
                Y1=m;
             end
          end
       end
       if(peakfound1==1 && Rn(m,n)>0 )
          for j=-range:range
             if(Gp(m+j,n)>0)
                peakfound2=1;
             end
          end
       end
       if(peakfound2==1 && Rn(m,n)>0)
          for j=-range:range
             if(Gn(m+j,n)>0)
                peakfound3=1;
                Y2=m;
             end
          end
```

```
        end
        if(peakfound3==1)
           for j=Y1:-1:Y2
              X(j,n)=offset;
            end
           offset=offset+1;
           peakfound1=1;peakfound2=0;peakfound3=0;
           Y1=m;
        end
     end
  end
X=X.*(2*pi);
ph=X+ph;
for n=1:n
    ph(:,n)=ph(:,n)/(max(ph(:,n)));
end
ph=ph*(2*pi);
F=9;
ph=imfilter(ph,ones(F,F)/(F*F));
ph=ph/(max(max(ph)));
ph=ph*(2*pi);
PU=ph;

% figure(1),imagesc(PU),colormap gray;
% figure(2) , plot(100:900,PU(100:900,500));

%}
```

LinearInterpolation

```
%{ This function fills out the holes or blank spots in the snake images

function Out=Peaks_Linearfiltering(S,h,v)
side=floor(((v-1)/2));
[M,N]=size(S);
I=zeros(M,N);
m1=0;m2=0;n1=0;n2=0;
for m=1:M
    for n=1:N
        foundnext=0;
        n1=0;n2=0;
        if(S(m,n)>0)
           m1=m; n1=n;
           for u=1:min(h,N-n)
              for v=0:min(v,M-m)
                 mx=m1-side+v;
                 nx=n1+u;
```

```
            if(S(mx,nx)>0 && foundnext==0)
              m2=mx;
              n2=nx;
              foundnext = 1;
            end
          end
        end
      end
      if(n1>0 && n2>0)
        a=(m2-m1)/(n2-n1);
        b=m1-(a*n1);
        for x=n1:n2
          y =round((a*x)+b);
          if(y>0 && y<N)
            S(y,x)=1;
          end
        end
      end
   end
end
Out=S;
%}
```

PhasetoWorldCoordinatesCalculation

```
%{ Program for 3D reconstruction of the object from obtained phase unwrap and
calibration Information

L=667.75;       % L- indicates reference plane position (on which object is placed)
d=203.2;        % d- distance between the camera  and projector
deltah=76.2;    % deltah - known distance between initial reference and moved planed
positions.

[M,N]= size(PUR);
ph_temp=zeros(M,N);
B=zeros(M,N);
BC1=zeros(M,N);
BC2=zeros(M,N);
H1=zeros(M,N);
H2=zeros(M,N);
%Loop to calculate the difference in phase between Reference and Moved
%plane positions
 for x=1:M               % m=vertical row number.
   for y=1:N            %n=space along columns ie. horizontal space.
    ph_temp(x,y)=PUM(x,y)-PUR(x,y);
    B(x,y)=deltah/((ph_temp(x,y)*(L/d))-(deltah*ph_temp(x,y)/d));
      end
```

```
 end

%Height of Moved plane w.r.t to Inital Reference plane position%
for x=1:M
   for y=1:N
   BC1(x,y)=B(750,700)*(PUM(x,y)-PUR(x,y));
   H1(x,y)=(BC1(x,y)*(L/d))/(1+BC1(x,y)/d);

   end
end

%Height of Curved Surface w.r.t to Inital Reference plane position%

for x=1:M
   for y=1:N
   BC2(x,y)=B(750,700)*((PUC(x,y)-PUR(x,y)));
   H2(x,y)=(BC2(x,y)*(L/d))/(1+BC2(x,y)/d);

   end
end

% Scale-factor measured as mm/pixel on the object to scale x and y axis properly%
scale_factor = 121.44/1420;
 x=zeros(M,N);
 for j=1:N
        x(:,j)=j*scale_factor;
 end
 y=zeros(M,N);
 for j=1:M
        y(j,:)=j*scale_factor;
 end
  z=zeros(M,N);
 z=H2;
 out=H2;
  temp=ones(M,N);
 temp=temp*255;
 imageI=uint8(temp);
 temp1=ones(M,N);
 temp1(find(abs(z)<200))=z(find(abs(z)<200));
 z=temp1;
 temp1=(z-(min(min(z))))/(max(max(z)));
 imageC=uint8(255*temp1);

 %}
```

References

[1] Jarvis R.A, “A Perspective on Range Finding Techniques for Computer Vision,” *IEEE Trans. on Pattern Analysis and Machine Intelligence* 5(2), 122-139, 1983.

[2] F. Chen, G. M. Brown, and M. Song, “Overview of three-dimensional shape measurement using optical methods,” *Opt. Eng.* 39**(**1) 10–22, 2000.

[3] S. Tang and Y. Y. Hung, “Fast profilometer for the automatic measurement of 3-D object shapes,” *Appl. Opt.* 29(20), 3012–3018, 1990.

[4] I. J. Batlle, E.Mouaddib and J.Salvi “Recent Progress in coded structured light as a technique to solve the correspondence problem”, *Pattern Reorganization,* 31(7), 963-982, 1998.

[5] Salvi J, Garcia R, Matabosch, C, “Overview of coded light projection techniques for automatic 3D profiling,” *Proceedings of the 1003 IEEE International Conference on Robotics &Automation* Pages(s) 133- 138 2003.

[6] V. Srinivasan, H.C. Liu, M. Halioua, “Automated phase- measuring profilometry of 3-D diffuse objects”, *Applied Optics*, 23(18), 3105-8, 1984.

[7] R. C. Daley and L. G. Hassebrook, "Channel capacity model of binary encoded structured light-stripe illumination," *Appl. Opt*. 37, 3689-3696 (1998)

[8] L.G.Hassebrook, R.C.Daley and W.Chimitt, “Application of communication theory to high speed structured light illumination” in *proceedings of SPIE*, Harding and Svetkoff,Eds.,October 1997,pp.102-113.

[9] Jielin Li, L.G. Hassebrook and Chun Guan, “Optimized Two-Frequency Phase-Measuring-Profilometry Light-Sensor Temporal-Noise Sensitivity,” *JOSA A*, 20(1), 106-115, (2003).

[10] V.G.Yalla and L.G. Hassebrook “Very high resolution 3D surface scanning using multi-frequency phase measuring profilometry” in *Proceedings of SPIE*, Vol. 5798, 44, 2005.

[11] Veeraganesh Yalla, "Optimal Phase Measuring Profilometry Techniques for Static and Dynamic 3D Data Acquisition," PhD Dissertation, University of Kentucky, Lexington, KY, USA, 2006.

[12] Keller K and Ackerman J., Real-time structured light depth extraction, SPIE *Photonics West - Electronic Imaging*, 3158, pp. 11-19, 2000.

[13] P. Vuylsteke, A. Oosterlinck, Range image acquisition with a single binary-encoded light pattern, IEEE Trans. Pattern Anal. and Mach. Intell. 12 (2) 148–164, 1990.

[14] P. M. Griffin, L. S. Narasimhan, S. R. Yee, Generation of uniquely encoded light patterns for range data acquisition, Pattern Recognition 25 (6) 609–616, 1992.

[15] G. Goli, C. Guan, L. G. Hassebrook, and D. L. Lau, “Video rate three dimensional data acquisition using composite light structure pattern,” Tech. Rep. CSP 02-002, University of Kentucky, Department of Electrical and Computer Engineering, Lexington, KY USA , 2002.

[16] Chun Guan, "Composite Pattern for Single Frame 3D Acquisition," PhD Dissertation, University of Kentucky, Lexington, Ky, USA, 2004.

[17] L.G Hassebrook, DL Lau, “Structured Light Illumination Strategy INTRODUCTION OF LOCK AND HOLD STRUCTURED LIGHT ILLUMINATION,” University of Kentucky EE Report #CSP 06-004, 2-20-06, Revised 5-26-06.

[18] C.J.Casey, “Structured Light Motion Capture”, MS thesis, University of Kentucky, Lexington, KY, USA, December 2008.

[19] Oleksandr A. Skydan, Michael J. Lalor, and David R. Burton, "Technique for phase measurement and surface reconstruction by use of colored structured light," *Applied Optics*, 41(29):6104-17, 2002.

[20] K.Boyer and A.Kak, “color-encoded structured light for rapid active ranging” *IEEE Trans.Pattern.Anal.Mach.Intell*. 9, 2724-2729, 1987.

[21] Tsalakanidou, F., Forster, F., Malassiotis, S., and Strintzis, M. G. 2005. Real-time acquisition of depth and color images using structured light and its application to 3D face recognition. *Real-Time Imaging* 11, 5-6 , 358-369, Oct. 2005.

[22] J.Salvi, J.Batlle, and E.Mouaddib, “A robust-coded pattern projection for dynamic 3d scene measurement”, Pattern Recogn.Lett.19 (11), 1-55-1065, 1998.

[23] J.Tajima and M.Iwakawa, “3-D data acquisition by rainbow range finder”, in *Intl. Conf.pm Patterm Recognition*, pp.309-313, 1990.

[24] Z.J.Geng, “Rainbow three-dimensional camera: new concept of high-speed three-dimensional vision systems”, *Opt.Eng*.35 (2), 376-383, 1996.

[25] W. Liu, Z. Wang, G. Mu, and Z. Fang, “Color-coded projection grating method for shape measurement with a single exposure,” *Appl. Opt.* **39(**20), 3504–3508, 2000.

[26] P. S. Huang, Q. Hu, F. Jin, and F. P. Chiang, "Color-encoded digital fringe

Projection technique for high-speed three-dimensional surface contouring," *Opt. Eng.*38(6), 1065–1071, 1999.

[27] Jaihui Pan, Peisen S. Huang, and Fu-Pen Chiang, “Color-phase shifting technique for three-dimensional shape measurement,” *Optical Engineering* Volume 45, Issue 1, 013602, January 2006.

[28] Wei-Hung Su, “Color-encoded fringe projection for 3D shape measurements,” *Opt.Express* 15, 13167-13181, 2007.

[29] C. Guan, L. Hassebrook, and D. Lau, "Composite structured light pattern for three-dimensional video," *Opt. Express 11*, 406-417, 2003.

[30] J. Li, H. Su, and X. Su, "Two-frequency grating used in phase-measuring profilometry," Appl. Opt. 36, 277-280, 1997.

[31]**http://www.kodak.com/global/en/service/slideProj/ektagraphic/ownerManual/ektgToc.shtml.**

[32] A. Robinson, L. Alboul, and M. Rodrigues. “Methods for indexing stripes in uncoded structured light scanning systems,” *Journal of WSCG*, 12(3):371-378, February 2004.

Vita

Neelima Mandava was born on 11th May 1983 in Guntur, India. She was awarded Bachelors of Engineering in Electronics from National Institute of technology in 2006. She worked as project developer in Indus Research and Development Ltd from May 2001 to July 2002. She was a Research Assistant at University of Kentucky Signal and Image Processing Lab, from May 2007 to October 2008.

Neelima Mandava